Host-induced bacterial cell wall decomposition mediates pattern-triggered immunity in Arabidopsis

Xiaokun Liu, Heini M Grabherr, Roland Willmann, Dagmar Kolb, Frédéric Brunner, Ute Bertsche, Daniel Kühner, Mirita Franz-Wachtel, Bushra Amin, Georg Felix, Marc Ongena, Thorsten Nürnberger, Andrea A Gust

DOI: http://dx.doi.org/10.7554/eLife.01990

Cite as: eLife 2014;10.7554/eLife.01990

Received: 2 December 2013
Accepted: 20 June 2014
Published: 23 June 2014

Host-induced bacterial cell wall decomposition mediates pattern-triggered immunity in *Arabidopsis*

Xiaokun Liu[1†], Heini M. Grabherr[1†], Roland Willmann[1], Dagmar Kolb[1], Frédéric Brunner[1], Ute Bertsche[2], Daniel Kühner[2], Mirita Franz-Wachtel[3], Bushra Amin[4], Georg Felix[1], Marc Ongena[5], Thorsten Nürnberger[1]*, Andrea A. Gust[1]*

[1]Department of Plant Biochemistry, Center for Plant Molecular Biology (ZMBP), University of Tübingen, Tübingen, Germany; [2]Department of Microbial Genetics, University of Tübingen, Tübingen, Germany; [3]Proteome Center Tübingen, University of Tübingen, Tübingen, Germany; [4]Medical and Natural Sciences Research Centre, University of Tübingen, Tübingen, Germany; [5]Wallon Centre for Industrial Biology, University of Liege-Gembloux Agro-Bio Tech, Gembloux, Belgium

[†]These authors contributed equally

*For correspondence: andrea.gust@zmbp.uni-tuebingen.de (AAG); thorsten.nuernberger@zmbp.uni-tuebingen.de (TN), phone +49 7071 2976655 or +49 7071 2976658, fax +49 7071 295226

Competing interests: The authors declare that no competing interests exist.

Abstract

Peptidoglycans (PGN) are immunogenic bacterial surface patterns that trigger immune activation in metazoans and plants. It is generally unknown, how complex bacterial structures, such as PGN, are perceived by plant pattern recognition receptors (PRR) and whether host hydrolytic activities facilitate decomposition of bacterial matrices and generation of soluble PRR ligands. Here, we show that *Arabidopsis thaliana* upon bacterial infection or exposure to microbial patterns produces a metazoan lysozyme-like hydrolase (lysozyme 1, LYS1). LYS1 activity releases soluble PGN fragments from insoluble bacterial cell walls and cleavage products are able to trigger responses typically associated with plant immunity. Importantly, *LYS1* mutant genotypes exhibit super-susceptibility to bacterial infections similar to that observed on PGN receptor mutants. We propose that plants employ hydrolytic activities for the decomposition of complex bacterial structures, and that soluble pattern generation might aid PRR-mediated immune activation in cell layers adjacent to infection sites.

Introduction

Activation of antibacterial defenses in multicellular eukaryotic organisms requires recognition of bacterial surface patterns through host-encoded pattern recognition receptors (PRR) (Boller and Felix, 2009, Chisholm et al., 2006, Ishii et al., 2008, Jones and Dangl, 2006, Segonzac and Zipfel, 2011, Vance et al., 2009, Broz and Monack, 2013, Monaghan and Zipfel, 2012, Stuart et al., 2013). Immunogenic microbial signatures are collectively referred to as pathogen or microbe-associated molecular patterns (PAMPs/MAMPs) (Janeway and Medzhitov, 2002). Bacteria-derived PAMPs, such as lipopolysaccharides (LPS) or flagellins possess immunity-stimulating activities in metazoans and plants, suggesting that the ability to sense bacterial surface structures and mount immunity is conserved across lineage borders (Boller and Felix, 2009, Nürnberger et al., 2004).

Likewise, peptidoglycans (PGNs) are major building blocks of the cell walls of Gram-positive and Gram-negative bacteria that have been shown to trigger host immune responses in mammalians, insects and plants (Dziarski and Gupta, 2005, Erbs et al., 2008, Gust et al., 2007, Kurata, 2014). Structurally, PGNs are heteroglycan chains that are composed of polymeric alternating β (1,4)-linked *N*-acetylglucosamine (GlcNAc) and *N*-acetylmuramic acid (MurNAc) residues (Glauner et al., 1988, Schleifer and Kandler, 1972). Such chains are interconnected by oligopeptide bridges, which form a coordinate meshwork thereby providing structural integrity to the bacterial envelope. Recognition of different PGN substructures in animal hosts is brought about by structurally diverse PRRs, such as nucleotide-binding oligomerization domain-containing proteins (NODs), peptidoglycan recognition proteins (PGRPs/PGLYRPs), scavenger receptors, or Toll-like receptor TLR2 (Dziarski and Gupta, 2010, Kurata, 2014, Müller-Anstett et al., 2010, Royet and Dziarski, 2007, Strober et al., 2006, Magalhaes et al., 2011). In plants, a tripartite PGN recognition system at the plasma membrane of *Arabidopsis thaliana* with shared functions in PGN sensing and transmembrane signalling was recently described (Willmann et al., 2011). This system comprises Lysin motif (LysM) domain proteins LYM1 and LYM3 for PGN ligand binding and the transmembrane LysM receptor kinase CERK1 that is likely required for conveying the extracellular signal across the plasma membrane and for initiating intracellular signal transduction. All three proteins were shown to be indispensable for PGN sensitivity and to contribute to immunity to bacterial infection (Willmann et al., 2011), which is in agreement with their proposed role as PGN sensor system. More recently, a similar PGN perception system made of LysM domain proteins LYP4 and LYP6 has been reported from rice (Liu et al., 2012a).

Microbial patterns such as bacterial PGN, LPS, flagellin, or fungal chitin harbor immunogenic epitopes that are parts of supramolecular structures building microbial surfaces (Boller and Felix, 2009, Kumar et al., 2013, Newman et al., 2013, Pel and Pieterse, 2013). It is therefore assumed that recognition by host PRRs most likely requires the presence of soluble, randomly structured ligands derived from a complex matrix. X-ray structure-based insight into the binding of bacterial flagellin to the *Arabidopsis* receptor complex FLS2/BAK1 or of fungal chitin to the *Arabidopsis* receptor CERK1 are in support of this view (Liu et al., 2012b, Sun et al., 2013, Willmann and Nürnberger, 2012). Moreover, the existence of fungal LysM effector proteins that scavenge soluble chitin fragments thus preventing recognition by plant PRRs suggests already that mechanisms releasing these soluble fragments from fungal cell walls must exist (de Jonge et al., 2010). Most often, however, it is an open question whether soluble ligand presentation to eukaryotic host PRRs is the result of spontaneous decomposition of microbial extracellular matrix during infection or, alternatively, whether host-derived factors contribute to the generation of immunogenic ligands for PRR activation. For example, only monomers of bacterial flagellin induce immune responses through human TLR5 whereas filamentous flagella, in which the immunogenic flagellin structure is buried and thus is not accessible to TLR5, do not (Smith et al., 2003). It was proposed that a number of circumstances cause flagellin monomer release from intact flagella. For instance, *Caulobacter crescentus* deliberately ejects its flagellum once it is no longer required for the bacterial life cycle (Jenal and Stephens, 2002). Moreover, during infection *Pseudomonas aeruginosa* produces rhamnolipids which act as surfactants and cause flagellin-shedding from intact flagella, resulting in a more pronounced immune response (Gerstel et al., 2009). Alternatively, host factors, such as proteases, or environmental conditions such as pH, temperature or bile salts have been proposed to mediate shearing of flagella from bacterial surfaces (Ramos et al., 2004). Likewise, recognition of PGN by intracellular receptors, such as mammalian NOD1 and NOD2, or by plasma membrane receptors, such as mammalian TLR2 or plant LYM1, LYM3 and CERK1 (Müller-Anstett et al., 2010, Sorbara and Philpott, 2011, Willmann et al., 2011) is facilitated by soluble ligands. Animal lysozymes have been implicated in PGN hydrolysis, bacterial lysis, and host immunity (Callewaert and Michiels, 2010) likely through partial PGN degradation and generation of soluble ligands for PGN sensors (Cho et al., 2005, Dziarski and Gupta, 2010, Davis et al., 2011).

In plants, knowledge on the mode of release of immunogenic fragments from microbial extracellular structures and their contribution to plant immunity is lacking. We here describe a plant

93 enzyme activity (LYS1) that hydrolyzes β (1,4)-linkages between N-acetylmuramic acid and N-
94 acetylglucosamine residues in peptidoglycan and between N-acetylglucosamine residues in
95 chitooligosaccharides, thus closely resembling metazoan lysozyme (EC 3.2.1.17). Importantly, PGN
96 breakdown products produced by LYS1 are immunogenic in plants, and *LYS1* mutant genotypes were
97 immunocompromised upon bacterial infection. Our findings suggest that plant enzymatic activities,
98 such as LYS1, are capable of generating soluble PRR ligands that might contribute to the activation of
99 immune responses in cells at and surrounding the site of their generation. We also infer that
100 eukaryotic hosts more generally make concerted use of PGN-hydrolytic activities and of pattern
101 recognition receptors in order to cope with bacterial infections.
102
103 **Results**
104 **Arabidopsis PGN binding proteins LYM1 and LYM3 are devoid of PGN-hydrolytic activity**
105 Soluble oligomeric PGN fragments have previously been shown to stimulate plant immune responses
106 in *Arabidopsis* (Erbs et al., 2008, Gust et al., 2007, Willmann et al., 2011). As some metazoan
107 peptidoglycan recognition proteins (PGRP) harbor PGN-degrading enzyme activities (Bischoff et al.,
108 2006, Dziarski and Gupta, 2010, Gelius et al., 2003, Kurata, 2010, Wang et al., 2003) we tested
109 whether recombinant *Arabidopsis* PGN binding proteins LYM1 and LYM3 were able to catalyze PGN
110 degradation. For this, we have employed a standard lysozyme assay (Park et al., 2002) that is based
111 on reduced turbidity in suspensions of Gram-positive *Micrococcus luteus* cell wall preparations due to
112 PGN degradation. PGN-degrading activity of hen egg-white lysozyme served as positive control in
113 these assays. As shown in Figure 1A, lysozyme, but not recombinant LYM1 or LYM3, displayed cell
114 wall-degrading lytic activity, suggesting that the latter are unable to release PGN fragments from
115 bacterial cell walls. This is in agreement with a lack of sequence similarities between LYM1 or LYM3
116 and known metazoan PGN hydrolytic activities. We therefore conclude that LYM1 and LYM3
117 constitute plant PGN sensors that appear to be functionally related to non-enzymatic mammalian or
118 *Drosophila* PGRPs (Bischoff et al., 2006, Cho et al., 2005, Dziarski and Gupta, 2010, Kurata, 2010).
119
120 ***LYS1* expression is activated upon bacterial infection**
121 Lysozymes (EC 3.2.1.17) hydrolyze β (1,4)-linkages between N-acetylmuramic acid and N-
122 acetylglucosamine residues in peptidoglycans and between N-acetylglucosamine residues in
123 chitodextrins (http://enzyme.expasy.org/EC/3.2.1.17). Plant genomes do not encode lysozyme-like

proteins, but many plant species produce lysozyme-like enzyme activities, such as chitinases (EC 3.2.1.14) (Audy et al., 1988, Sakthivel et al., 2010). Plant chitinases fall into five classes (I-V, Figure 1B) (Passarinho and de Vries, 2002) and are grouped into structurally unrelated families 18 and 19 of glycosyl hydrolases, respectively (Henrissat, 1991). Chitinases belonging to family 18 of glycosyl hydrolases are ubiquitously found in all organisms whereas chitinases of glycosyl hydrolase family 19 are found almost exclusively in plants. Class III chitinases (glycosyl hydrolase family 18) represent bifunctional plant enzymes with lysozyme-like activities. One such enzyme, hevamine from rubber tree, *Hevea brasiliensis* (Beintema et al., 1991), has been shown to hydrolyze PGN and the structurally closely related β (1,4)-linked GlcNAc homopolymer chitin *in vitro* (Bokma et al., 1997).

To explore host-mediated PGN degradation and its possible implication in plant immune activation we have addressed the only class III chitinase (that we named LYS1, At5g24090) encoded by the *Arabidopsis* genome (Passarinho and de Vries, 2002) (Figure 1B). Bacterial infection of *Arabidopsis* plants stably expressing a *pLYS1::GUS* construct revealed that *LYS1* gene expression is enhanced upon infection with host non-adapted *P. syringae* pv. *phaseolicola* (*Pph*) or disarmed host adapted *Pseudomonas syringae* pv. *tomato* (*Pto*) DC3000 hrcC^{-}. Likewise, expression of the immune response marker, pathogenesis-related protein 1 (*PR1*) was enhanced by the same treatment (Figure 1C). Failure to detect *LYS1* expression in plants infected with virulent host adapted *Pto* DC3000 suggests bacterial effector-mediated suppression that is reminiscent of that observed for PGN receptor proteins LYM1 and LYM3 (Willmann et al., 2011) as well as numerous other immunity-associated genes (Kemmerling et al., 2007, Postel et al., 2010). *LYS1* gene expression is not only triggered upon bacterial infection, but was also observed upon treatment with different MAMPs including bacterial flagellin, lipopolysaccharide (LPS) or PGN preparations (Figure 1D), similar to the immune marker gene *Flagellin-responsive Kinase 1* (*FRK1*). Altogether, infection-induced *LYS1* transcriptional activation suggests that the LYS1 protein is implicated in immunity to bacterial infection.

LYS1 is a plant lysozyme

To analyse enzymatic properties of LYS1, recombinant protein production was attempted. Overexpression in *E. coli* failed to produce active enzyme and LYS1 production in eukaryotic *Pichia pastoris* entirely failed to produce recombinant protein (not shown). Therefore, we resorted to generate *p35S::LYS1-GFP*-overexpressing (*LYS1*^{OE}) plants (Figures 2A and 2B). Notably, LYS1-GFP was glycosylated (Figure 2C), possibly explaining the failure to produce enzymatically active LYS1 protein

in *E. coli*. Expression of the GFP-fusion protein in Arabidopsis plants was accompanied by substantial proteolytic cleavage resulting in a predominant release of a protein with an approximate molecular mass of 35 kDa, most likely representing untagged LYS1 (Figure 2B). Analysis of this major cleavage product by LC-MS/MS after tryptic in-gel digestion and by peptide mass fingerprint not only confirmed the identity of LYS1 in this band but also yielded peptides spanning the whole protein sequence, except for the first 53 amino acids (data not shown), thus indicating cleavage of the LYS1-GFP fusion protein between LYS1 and GFP.

Three mutant lines with T-DNA insertions in the LYS1 gene were available from the Nottingham Arabidopsis Stock Centre. However, neither the insertion in the 5' untranslated region nor the insertions in the first intron and at the end of the last exon of the coding region abolished formation of the *LYS1* transcript. (Figure 3-figure supplement 1). As an alternative to 'knock out' lines *LYS1* knock-down lines (*LYS1*^{KD}) were produced by artificial micro RNA technology (Schwab et al., 2006) (Figure 3). As proven by RT-qPCR, we obtained two genetically independent *LYS1*^{KD} lines with residual transcript levels not exceeding 10 % of those detected in wild-type plants (Figure 3C). In contrast, the transcription of potential off-target genes was not affected (Figure 3C). Protein extracts derived from transgenic plants were tested for chitinolytic activity by employing 4-methylumbelliferyl β-D-N, N', N''-triacetylchitotriose (4-MUCT) as substrate. Leaf protein extracts from *LYS1*^{OE} plants exhibited significant chitinase activity when compared to a *Streptomyces griseus* chitinase control (Figure 4A). In contrast, wild type and *LYS1*^{KD} plants exhibited only marginal chitinase activities. Likewise, using 4-MUCT in a gel electrophoretic separation-based chitinase assay produced a zymogram in which enzyme activity was solely detectable in protein extracts obtained from *LYS1*^{OE} plants, but not in those from control plants expressing secreted GFP (*secGFP*) (Figure 4B). Thus, LYS1 indeed harbors the predicted chitinase activity. As 4-MUCT is also a typical substrate for lysozymes (Brunner et al., 1998), this was the first indication that LYS1 might also harbor lysozyme activity. Next, leaf protein extracts from *LYS1*^{OE} plants were tested for their ability to solubilize complex PGN presented by intact Gram-positive *Micrococcus luteus* cells and to cleave preparations of complex, insoluble *Bacillus subtilis* PGN. Again, protein extracts from *LYS1*^{OE} plants exhibited significant PGN-degrading activity, whereas wild type and *LYS1*^{KD} plants showed basal activity levels only (Figures 4C and 4D). Likewise, PGN-solubilizing activity profiles of protoplast suspensions derived from these transgenics confirmed significant PGN-degrading activity of *LYS1*^{OE} plants (Figure 4E).

To determine specific enzyme activities, untagged LYS1 was purified from *LYS1*^{OE} *Arabidopsis* lines by fast protein liquid chromatography and used for enzyme assays. The 4-MUCT assay yielded a K_m of 70 ± 14 µM and a V_{max} of 378 ± 42 µM min^{-1} mg^{-1} for LYS1, and a K_m of 53 ± 27 µM and a V_{max} of 397 ± 145 µM min^{-1} mg^{-1} for commercial *S. griseus* chitinase. Using the turbidity assay with *M. luteus* cell wall preparations a K_m of 18,2 ± 2,5 mg/ml and V_{max} of 4,4 ± 0,6 mg mg^{-1} min^{-1} were obtained for LYS1, and a K_m of 8,4 ± 0,8 mg/ml and V_{max} of 192 ± 120 mg mg^{-1} min^{-1} for commercial hen egg white lysozyme. The K_m values for LYS1 are thus comparable to the commercial enzymes.

As shown in Figure 4E, the majority of LYS1 activity was found in the supernatant of the protoplasts, suggesting an apoplastic localization of LYS1. To confirm this localization, we prepared apoplastic washes from *LYS1*^{OE} Arabidopsis lines. Both the LYS1-GFP fusion protein as well as free LYS1 was detectable in concentrated apoplastic fluids whereas the cytoplasmic mitogen-activated protein kinase MPK3 was only present in the total leaf protein samples (Figure 4-figure supplement 1A). Moreover, transient expression in the heterologous plant system *Nicotiana benthamiana* of the *p35S::LYS1-GFP* construct resulted in labelling of the cell periphery, whereas expression of a construct lacking the *LYS1* signal peptide-encoding sequence yielded labelling of intracellular structures (Figure 4-figure supplement 1B). Use of the fluorescent dye FM4-64, a plasma membrane and early endosome marker (Bolte et al., 2004), revealed that LYS1 signals co-localized to a large extent with the plasma membrane (Figure 4-figure supplement 1B). Thus, LYS1 likely operates in close vicinity of the plant surface. Indeed, previous identification within the *Arabidopsis* cell wall proteome (Kwon et al., 2005) suggests that LYS1 acts in the plant apoplast. Since the plant apoplast is an acidic compartment (pH 5-6) (Schulte et al., 2006), we investigated whether LYS1 is active at physiologically relevant pH conditions. For this, the *M. luteus* cell wall-degrading activity of an *LYS1*^{OE} leaf extract was determined at different pH values. Although active at pH values ranging from 3.2 to 7.2, a pronounced maximum of LYS1 activity was detected around pH 6 that coincided with the apoplastic pH of plant cells (Figure 4F).

To further confirm LYS1 glucan hydrolytic activity, an epitope-tagged *LYS1* fusion construct was transiently expressed in *N. benthamiana* (Figure 5A). Similar to the Arabidopsis *LYS1*^{OE} leaf extracts also extracts from *p35S::LYS1-myc* expressing *N. benthamiana* leaves displayed *in-gel* chitinolytic activity (Figure 5B) compared to extracts from control leaves expressing the viral silencing

suppressor p19 only. Likewise, *N. benthamiana* protein extracts containing LYS1-myc were able to cleave preparations of complex, insoluble *B. subtilis* PGN (Figure 5C).

In sum, we provide biochemical evidence that LYS1 harbors hydrolytic activity for chitin as well as for PGN of the lysine-type (*M. luteus*) and diaminopimelic acid-type (*B. subtilis*). Importantly, LYS1 failed to exhibit activity on cellobiose as a substrate, indicating it might have no cellulose activity (Figure 4-figure supplement 2). Thus, LYS1 resembles enzymatic activities reported for metazoan lysozymes and should be classified as lysozyme (EC 3.2.1.17) instead of chitinase (EC 3.2.1.14).

LYS1 generates plant immunogenic PGN fragments

To analyze immunogenic activities of PGN cleavage products generated by LYS1, untagged LYS1 was purified from *LYS1*^{OE} *Arabidopsis* lines by FPLC and used for degradation of *B. subtilis* PGN. Solubilized PGN fragments found in the supernatant of LYS1-digested PGN were subsequently analyzed by high performance liquid chromatography (Figure 6A). Only few peaks could be detected in the supernatant of PGN incubated with a buffer control or with heat-inactivated LYS1. In contrast, PGN-digests produced by native LYS1 yielded several characteristic peaks that were also detectable in the supernatants of PGN preparations treated with mutanolysin, which has been shown to cleave O-glycosidic bonds between GlcNAc and MurNAc residues in complex PGN (Yokogawa et al., 1975). LYS1-generated PGN-fragments were subsequently tested for their ability to trigger plant immunity-associated responses (Figures 6B-D). First, supernatants of PGN preparations treated with either native or heat-denatured LYS1 were used to trigger immune marker gene *FRK1* expression in *Arabidopsis* seedlings. Importantly, only supernatants from PGN-digests produced by native LYS1 or mutanolysin induced *FRK1* expression whereas buffer controls or digests produced by heat-inactivated LYS1 did not release immunogenic soluble fragments from complex PGN (Figure 6B). Notably, activation of immune responses by LYS1-generated PGN-fragments was dependent on Arabidopsis PGN receptor complex components LYM1, LYM3 and CERK1 as the respective mutant genotypes failed to respond to immunogenic PGN fragments (Figure 6B). Second, we tested whether LYS1-generated PGN fragments were able to trigger an immunity-associated response, medium alkalinization, in rice cell suspensions. This plant was chosen for testing as a PGN receptor system very similar to that in *Arabidopsis* has recently been reported (Liu et al., 2012a). As shown in Figure 6C, LYS1-released PGN-fragments triggered medium alkalinization in cultured rice cells, suggesting that immune defense stimulation by soluble PGN fragments is not restricted to *Arabidopsis* only.

We further investigated the kinetics of PGN fragment release from complex PGN. As shown in Figure 6D, release of immunogenic PGN-fragments into solution occurred rapidly within 10 min of incubation with native LYS1. Incubation of complex PGN with LYS1 yielded the highest immunogenic activity of the digest supernatant after 30 min, suggesting that at that time point the maximum amount of immunogenic PGN fragments was generated. However, prolonged incubation with LYS1 again resulted in a loss of activity with overnight digestion completely abolishing stimulatory activity of the PGN digest. We assume that LYS1 is capable of releasing immunogenic fragments from complex PGN, but extensive or complete digest into PGN-monomers or small PGN fragments appears to abolish the immunogenic activity of PGN fragments. This result is in accordance with our previous observations that prolonged digestion of PGN with mutanolysin diminishes its defense-inducing activity (Gust et al., 2007).

LYS1 is required for plant immunity towards bacterial infections

To examine the physiological role of LYS1 in plant immunity, *LYS1*^{OE} and *LYS1*^{KD} lines were subjected to infection with various phytopathogens. As LYS1 harbors chitinase activity (Figures 4A, 4B and 5B) and as *LYS1* transcripts accumulate upon fungal infection (Samac and Shah, 1991), we first analyzed the role of LYS1 in immunity towards fungal infection. Leaves of transgenic *LYS1*^{OE} or *LYS1*^{KD} lines and WT plants were infected with the necrotrophic fungus *Botrytis cinerea*, and disease symptoms were monitored 2-3 days post infection. Fungal hyphal growth and necrotic leaf lesions at infection sites were detectable in all plant lines tested and hyphal outgrowth or cell death lesion sizes revealed no differences between WT, *LYS1*^{OE} or *LYS1*^{KD} lines (Figure 7). Likewise, infection with the necrotrophic fungus *Alternaria brassicicola* resulted in indistinguishable necrotic lesions in *LYS1*^{OE} and *LYS1*^{KD} transgenics compared to those observed in wild type control plants (Figure 8). Trypan blue staining and microscopical analysis of the infection sites did not reveal major differences in fungal hyphal growth among all lines tested (Figures 8B and 8C). Although disease indices at day 11 after infection were slightly increased in *LYS1*^{KD} lines (Figure 8D), such subtle differences were not statistically significant. In conclusion, we failed to detect a role for LYS1 in immunity to fungal infection with *B. cinerea* and *A. brassicicola* under our experimental conditions. However, these results cannot be generalized and LYS1 might still have a role under infection regimes other than the ones used here or it might be important for defense against other fungal pathogens.

To examine a role of LYS1 in immunity to bacterial infection, we infected wild type plants or *LYS1*^{KD} and *LYS1*^{OE} lines with virulent *Pto* DC3000. Two independent *LYS1*^{KD} lines exhibited hypersusceptibility to bacterial infection (Figure 9A), suggesting that lack of PGN-degrading activity results in reduced plant immunity. Likewise, immunity to hypovirulent *Pto* DC3000 Δ*AvrPto/PtoB* was compromised in these lines (Figure 9B). Moreover, expression of the immune marker gene *FRK1* upon administration of complex PGN was greatly impaired in the *LYS1*^{KD} mutants (Figure 9C). These findings suggest that the enzymatic activity of LYS1 on PGN contributes substantially to plant immunity against bacterial infection.

Unexpectedly, bacterial growth on *LYS1*^{OE} lines were also significantly enhanced as compared to those observed on wild type plants (Figures 9A and 9B). *FRK1* transcript accumulation upon administration of complex PGN was also strongly reduced in *LYS1*-overexpressors (Figure 9C). To exclude a direct effect of LYS1-overexpression on PGN receptor abundance, we examined transcript levels of *LYM1*, *LYM3* and *CERK1* but found no effect on the transcription of these receptor genes in the *LYS1*^{OE} lines (Figure 9 – figure supplement 1A). Also, CERK1 protein levels were unaltered in the *LYS1*^{OE} lines, whereas there was no CERK1 protein detectable in the *cerk1-2* mutant (Figure 9 – figure supplement 1A). Moreover, we included the *LYS1*^{OE}-3 line with only moderately increased *LYS1* transcript and protein levels in mature leaves (Figure 9 – figure supplement 1A and 1B). Susceptibility to *Pseudomonas* infection in the *LYS1*^{OE}-3 line was only slightly but not significantly increased ($p = 0{,}064$, Student's t-test). These results indicate that lowering *LYS1* expression levels, accompanied by lower LYS1 hydrolytic activity on PGN, brings down these lines close to wild-type. Thus, massive *LYS1* overexpression and loss-of-function mutations are phenocopies of each other, irrespective of the fact that *LYS1*^{KD} and *LYS1*^{OE} lines show dramatic differences in LYS1 enzymatic activities (Figure 4).

Altogether, we propose that LYS1 contributes to plant immunity to bacterial infection by decomposition of bacterial PGN and generation of soluble PGN-derived patterns that trigger immune activation in a LYM1-LYM3-CERK1 receptor-complex-dependent manner.

Discussion

It is generally little understood whether and how microbial patterns derived from complex extracellular assemblies, such as bacterial cell walls, are accessible to host PRRs for host immune activation in eukaryotes. This holds true for bacterial PGN, but also for other patterns including bacterial LPS,

flagellin or fungus-derived chitin or glucan structures, all of which have been ascribed triggers of innate immunity in metazoans and plants (Boller and Felix, 2009, Kumar et al., 2013, Newman et al., 2013, Pel and Pieterse, 2013). Limited insight into the 3D structure of ligand-PRR complexes as well as knowledge on ligand structural requirements for plant immune activation suggests that small ligand epitopes are crucial for binding to host PRRs (Liu et al., 2012b, Sun et al., 2013). It is thus generally assumed that soluble fragments derived of complex microbial matrices serve as ligands for host PRRs and subsequent immune activation in both lineages.

Two possible scenarios are discussed how soluble PGN fragments might be generated from macromolecular assemblies of cross-linked PGN. Firstly, during bacterial multiplication and cell wall biogenesis large portions of soluble PGN fragments are shed into the extracytoplasmic space, from which only 50-90% are recycled (Park and Uehara, 2008, Johnson et al., 2013, Reith and Mayer, 2011). This implies that imperfect recycling of bacterial walls might serve as a source of soluble ligands for host PRRs sensing PGN (Wyckoff et al., 2012, Boudreau et al., 2012). Indeed, muramylpeptides spontaneously shed by *Shigella flexneri* directly stimulate NOD1-dependent immune responses in mammalian immune cells, and bacterial mutants impaired in PGN recycling hyper-activate host immunity (Nigro et al., 2008). Secondly, host lysozyme activity has been demonstrated to generate soluble PGN ligands for NOD2 receptor-mediated immune activation and clearance of *Streptococcus pneumoniae* colonization in mice (Callewaert and Michiels, 2010, Clarke and Weiser, 2011, Davis et al., 2011). Importantly, Davis et al. (2011) established a role for host lysozymes in PGN release from bacteria in the absence of detectable bacterial lysis. Likewise, *Drosophila* Gram-negative bacteria-derived binding protein 1 (GNBP1) was shown to possess PGN-hydrolyzing activity and to deliver fragmented PGN to the PGN-sensor, PGRP-SA (Filipe et al., 2005, Wang et al., 2006). Altogether, both passive and active mechanisms of PGN decomposition appear to occur simultaneously during host pathogen encounters and might not be mutually exclusive.

We here report on a lysozyme-like enzyme (LYS1) that is produced in infected *Arabidopsis* plants and that is capable of generating soluble PGN fragments from complex bacterial PGN. LYS1 has been demonstrated to hydrolyze β (1,4)-linkages between N-acetylmuramic acid and N-acetylglucosamine residues in peptidoglycans and between N-acetylglucosamine residues in chitin oligomers thus closely resembling metazoan lysozymes. LYS1-generated fragments trigger immunity-associated responses in a PGN receptor-dependent manner. Activation of defenses has been further shown to occur in the two plants, Arabidopsis and rice, for which PGN perception systems have been

339 described to date (Liu et al., 2012a, Willmann et al., 2011). Importantly, *Arabidopsis* plants with
340 strongly reduced *LYS1* expression were impaired in immunity to bacterial infection, suggesting
341 strongly that LYS1 function is an important element of the immune system of this plant. Notably,
342 immuno-compromised phenotypes in *LYS1*^{KD} plants were comparable to those observed in either
343 *lym1 lym3* or *cerk1* PGN receptor mutant genotypes (Willmann et al., 2011). We further found that
344 plants overexpressing LYS1 were also susceptible to bacterial infections, suggesting that defined
345 LYS1 levels in wild-type plants are required for LYS1 immune function. The most compelling
346 explanation for this phenotype is that PGN hyper-degradation (in *LYS1*^{OE} plants) or lack of PGN
347 degradation (in *LYS*^{KD} mutants) are equally disadvantageous to plant immunity and that immune
348 activation in *Arabidopsis* requires oligomeric PGN fragments of a particular minimum degree of
349 polymerization (DP). This view is supported by our findings that prolonged digestion of PGN by LYS1
350 (Figure 6D) or by mutanolysin (Gust et al., 2007) abolished the immunogenic activity of PGN.
351 Likewise, immunogenic activities of fungal chitin or oomycete glucans have been reported to require
352 defined minimum ligand sizes with a minimum of DP > 5 (Cheong et al., 1991, Zhang et al., 2002). We
353 therefore propose that *LYS1* overexpression might result in PGN fragments of insufficient size,
354 thereby mimicking the physiological status in *LYS1*^{KD} mutants lacking major PGN hydrolytic activities.
355 Plants produce various carbohydrate-degrading hydrolytic enzyme activities, some of which
356 have been implicated in plant immunity to microbial infection, such as glucanases and chitinases (van
357 Loon et al., 2006). While it is often not entirely clear how these enzymes contribute to plant immunity it
358 is widely assumed that this is due to microcidal activities of these proteins. In our study, we have
359 shown that *Arabidopsis* LYS1 cleaves O-glycosidic bonds formed between GlcNAc (indicative of
360 chitinolytic activity) as well as those formed between GlcNAc and MurNAc (indicative of
361 peptidoglycanolytic activity). We have however been unable to demonstrate any deleterious effect of
362 LYS1 overexpression on fungal infections, suggesting that at least *B. cinerea* and *A. brassicicola* are
363 not affected by LYS1 function. Likewise, we have been unable to demonstrate direct bactericidal
364 activity of LYS1 to *Pseudomonas syringae* (not shown), suggesting that the positive role of LYS1 in
365 plant immunity to bacterial infection is not due to its direct inhibitory effect on bacterial fitness. This
366 view is further supported by the fact that *LYS1*^{OE} plants with strongly enhanced PGN hydrolytic activity
367 do not exhibit enhanced immunity to *Pseudomonas* infections, but become hyper-susceptible to
368 infection (Figure 9). We cannot rule out at this point LYS1-mediated bacterial lysis, which would likely
369 also result in the release of immunogenic PGN fragments. We would like to emphasize, however, that

our findings are in agreement with a predominant role of LYS1 in generation of PGN fragments that subsequently can trigger plant immunity via PRRs. Hence, plant LYS1 functionally resembles recently described mammalian lysozymes that were shown to generate soluble PGN fragments for PGN receptor NOD2 thereby mediating immunity to *S. pneumoniae* infection in mice (Davis et al., 2011).

LYS1 gene expression is strongly enhanced upon PAMP administration or bacterial infection while expression levels in naive plants are low. It is conceivable that the low constitutive LYS1 levels are sufficient to generate soluble PGN fragments from bulk PGN-containing bacterial walls which are then perceived via the LYM1-LYM3-CERK1 receptor complex. Possibly, the pathogen-inducible later increase in LYS1 activity could have further roles for generating diffusible signals that might serve innate immune activation not only in cells that are directly in contact with invading microbes, but in cell layers adjacent to infection sites.

A role for plant glycosyl hydrolases in immunogenic PAMP generation and immune activation has been proposed previously (Fliegmann et al., 2004, Mithöfer et al., 2000). An extracellular soluble bipartite soybean glucan binding protein (GBP) was shown to harbor 1,3-β-glucanase activity and binding activity for glucan fragments of DP > 6 derived of intact glucans. Complex glucans constitute major constituents of various *Phytophthora* species, many of which are plant pathogens (Kroon et al., 2011). It was hence suggested that during infection GBP endoglucanase activity produces soluble *Phytophthora*-derived oligoglucoside fragments as ligands for the high-affinity binding site within this protein (Fliegmann et al., 2004). While this study supported the concept of plant hydrolases tailor-making ligands for plant PRRs, causal evidence for the involvement of the endoglucanase activity in plant immunity was not provided.

Eukaryotic PGN recognition proteins (PGRP, PGLYRP) are conserved from insects to mammals, bind PGN and function in antibacterial immunity (Bischoff et al., 2006, Cho et al., 2005, Dziarski and Gupta, 2010, Kurata, 2010, Kurata, 2014). Some PGRP family members are non-enzymatic PRRs (NOD1, NOD2), while others possess PGN-degrading activities (Bischoff et al., 2006, Dziarski and Gupta, 2010, Gelius et al., 2003, Kurata, 2010, Wang et al., 2003). PGN-hydrolytic enzyme activities, such as lysozymes, have been ascribed functions in direct bacterial killing (Cho et al., 2005) and in generating soluble PGN fragments as ligands for PRRs (Wang et al., 2006, Davis et al., 2011). LYS1 constitutes the first plant lysozyme-type activity for which a role in host immunity has been established. LYS1 is capable of generating immunogenic fragments from complex PGN, which themselves serve as ligands for the LYM1-LYM3-CERK1-PGN recognition complex in *Arabidopsis*.

Noteworthy, LYM1 and LYM3 are PGN recognition proteins that lack apparent intrinsic PGN-degrading activity. Altogether, we conclude that metazoans and plants employ hydrolytic activities for the decomposition of bacterial PGN during host immune activation. In addition to the established role of PGN in pattern-triggered immune activation, host-mediated degradation of bacterial PGN constitutes another conserved feature of innate immunity in both lineages. However, as the molecular components involved differ structurally among phylae, both facets of PGN-mediated immunity might have evolved convergently.

Materials and methods

Plant growth conditions and infections

Arabidopsis thaliana Columbia-0 wild type and *Nicotiana benthamiana* plants were grown on soil as described (Brock et al., 2010). T-DNA insertion lines for *LYS1* (*lys1-1*, WiscDsLox387C11; *lys1-2*, SALK_095362; *lys1-3*, CSHL_ET14179) were obtained from the Nottingham Arabidopsis Stock Centre. The transgenic *pPR1::GUS* and *secGFP* lines and the *lym1 lym3* and *cerk1-2* mutants have been described previously (Teh and Moore, 2007, Shapiro and Zhang, 2001, Willmann et al., 2011). Rice (*Oryza sativa*) suspension cell cultures were grown in MS-medium (4.41 g/l MS salt, 6 % (w/v) succrose, 50 mg/l MES, 2 mg/l 2,4-D) at 150 rpm and sub-cultured every week. Bacterial strains *Pseudomonas syringae* pv. *tomato* DC3000 or *Pto*DC3000 Δ*AvrPto/AvrPto*, *A. brassicicola* isolate MUCL 20297 and *B. cinerea* isolate BO5-10 were grown and used for infection assays on *Arabidopsis* leaves of 4-5 week old plants as described previously (Kemmerling et al., 2007, Lin and Martin, 2005). To visualize plant cell death and fungal growth on a cellular level, infected plants were stained with trypan blue in lactophenol and ethanol as described (Kemmerling et al., 2007).

Materials

Flg22 peptide was described previously (Felix et al., 1999). The purification of *Pseudomonas syringae* pv. *tomato* PGN was performed as described previously (Willmann et al., 2011). *Micrococcus luteus* cell wall preparations and *Bacillus subtilis* PGN were purchased from Invivogen (San Diego, CA), Cecolabs (Tübingen, Germany) and Sigma-Aldrich (Hamburg, Germany). PGNs and LPS (from *Pseudomonas aeruginosa*, Sigma-Aldrich) were dissolved in water at a concentration of 10 mg/ml and stored at -20°C. Mutanolysin was purchased from Sigma-Aldrich.

Constructs and transgenic lines

Recombinant His6-LYM1 and His6-LYM3 were expressed in *E. coli* and purified as previously described (Willmann et al., 2011). As negative control, a protein purification using non-induced cultures harbouring the His6-LYM3 construct was performed.

For the *p35S::LYS1* fusion constructs, a 903 bp fragment of the *LYS1* coding sequence without STOP codon was cloned using the primers At5g24090gatF and At5g24090gatR (Table 1). In a second PCR the recombination sites of the inserts were completed using the Gateway™ adaptor primers attB1 and attB2 (Invitrogen, Darmstadt, Germany). The resulting fragments were then subcloned into pDONR201 (Invitrogen) by using the BP clonase reaction according to the manufacturer's protocol (Invitrogen) and inserted into the binary expression vectors pK7FWG2.0 (C-terminal GFP-tag) (Karimi et al., 2005, Karimi et al., 2002) or pGWB17 (C-terminal myc-tag) (Nakagawa et al., 2007) by using the LR clonase reaction following the manufacturer's protocol (Invitrogen). For the *pLYS1::GUS* reporter construct, a 1948 bp fragment of the *LYS1* promoter sequence was amplified from *Arabidopsis* Col-0 genomic DNA using the primers At5g24090gatF2 and At5g24090gatR2 (Table 1), extended in a second PCR with Gateway™ adaptor primers attB1 and attB2 and subcloned into pDONR207 (Invitrogen) before inserted into the binary expression vector pBGWFS7 (Karimi et al., 2005, Karimi et al., 2002).

For the generation of *pLYS1::GUS* and *p35S::LYS1-GFP* overexpression lines (*LYS1*^{OE}) wild type Col-0 plants were transformed. Stable transgenic lines were generated using standard *Agrobacterium tumefaciens*-mediated gene transfer by the floral dip procedure (Clough and Bent, 1998). Expression of GFP-fusion proteins was confirmed by immuno-blot analysis using an anti-GFP antibody (Acris Antibodies GmbH) and anti-tobacco class III chitinase antibody (kindly provided by Michel Legrand, IBMP Strasbourg, France). The histochemical detection of ß-glucuronidase (GUS) enzyme activity in whole leaves of *pLYS1::GUS* or *pPR-1::GUS* transgenic *Arabidopsis* (Shapiro and Zhang, 2001) was determined as described earlier (Gust et al., 2007).

Artificial microRNA-mediated gene silencing was used to specifically knock-down *LYS1* in the Col-0 background as mutant lines carrying T-DNA insertions in the *LYS1* gene were unavailable. The Web microRNA Designer (WMD; http://wmd.weigelworld.org) was used to select the primers At5g24090miR-s, At5g24090miR-a, At5g24090miR*s and At5g24090miR*s (Table 1) for the generation of an artificial 21mer microRNA (Schwab et al., 2005). The *LYS1*-specific amiRNA was then introduced into the vector miR319a pBSK (pRS300) by directed mutagenesis. Knock down of the

LYS1 transcript level in stably transformed Col-0 plants (*LYS1* knock-down line, $LYS1^{KD}$) was determined by quantitative RT-PCR using primers At5g24090Fq and At5g24090Rq listed in Table 1. Off-target genes were identified using the Web microRNA Designer and transcript levels of the four top hits were determined by qRT-PCR using primers listed in Table 1.

Transient protein expression

Agrobacterium tumefaciens-mediated transient transformation of *N. benthamiana* was performed as described (Brock et al., 2010). The leaves were examined for expression of tagged fusion proteins 3-4 days post infection. Expression of fusion proteins was confirmed by immuno-blot analysis using anti-myc antibodies (Sigma-Aldrich) and localization studies of GFP fusion proteins were carried out using a confocal laser-scanning microscope as described (Willmann et al., 2011).

LYS1 purification from $LYS1^{OE}$ plants

From 5 weeks old $LYS1^{OE}$ Arabidopsis plants 500 g leaf tissue was frozen in liquid nitrogen and ground to fine powder. After addition of buffer A (20 mM NaAc, pH 5.2, 0.01 % (v/v) β-Mercaptoethanol) the extract was incubated on ice overnight. After filtration through four layers of cheesecloth, the homogenate was centrifuged at 10,000 g for 30 min. The supernatant was loaded on a cation exchange column (SP Sepharose, GE Healthcare, München, Germany) equilibrated with buffer A. The column was washed with buffer A and proteins were eluted with a 0 to 1 M NaCl gradient in buffer A. The elution fractions were monitored for LYS1 activity with the 4-MUCT assay and protein purification was further confirmed by SDS-PAGE. 4-MUCT-active fractions were pooled and exchanged to buffer A using Vivaspin 3 kDa columns (GE Healthcare). Protein concentration was determined using the Bradford assay.

For LC-MS analysis, the Coomassie Blue-stained band of the major cleavage product of the purified LYS1-GFP sample was cut and and in-gel digested with trypsin, as described elsewhere (Borchert et al., 2010). LC-MS analyses of the peptides were done on an EasyLC nano-HPLC (Proxeon Biosystems) coupled to an LTQ Orbitrap Elite mass spectrometer (Thermo Scientific) as described elsewhere (Conzelmann et al., 2013). MS data were processed using the software suite MaxQuant, version 1.2.2.9 (Cox and Mann, 2008) and searched using Andromeda search engine (Cox et al., 2011) against a target-decoy *A. thaliana* database containing 33,351 forward protein sequences, the sequence of the LYS1-GFP fusion protein and 248 frequently observed protein contaminants. MS data

were processed twice, once considering only fully tryptic peptides and once considering only semi-tryptic peptides. In each case, two missed cleavage sites were allowed, carbamidomethylation of cysteine was set as fixed modification and N-terminal acetylation and methionine oxidation were set as variable modifications. Mass tolerance was set to 6 parts per million (ppm) at the precursor ion and 20 ppm at the fragment ion level. Identified peptide spectrum matches (PSM) were statistically scored by MaxQuant software by calculation of posterior error probabilities (PEP) (Käll et al., 2008) for each PSM. All PSMs having a PEP below 0.01 were considered as valid.

For MALDI-TOF-MS, protein digestion was performed as described (Amin et al., 2014, Maurer et al., 2013). Briefly, the Coomassie Blue-stained band of the major cleavage product of the FPLC-purified LYS1-GFP sample was cut from the gel and destained with 30 % (v/v) acetonitrile in 50 mM ammonium bicarbonate buffer. Disulfide bonds were reduced with 10 mM DTT, 50 mM iodoacetamide was used to alkylate the cysteines followed by overnight protein digestion with mass spectrometry grade trypsin (Promega, Manheim, Germany) at 37°C. The digests were acidified by the addition of TFA to a final concentration of 0.5 %. Extracted peptides were desalted and mixed with an equal volume of 2,5-dihydroxybenzoic acid for Reflex-IV MALDI-TOF-MS (Bruker Daltonics, Bremen, Germany) measurements. Each spectrum was processed internally for trypsin autolysis before database search. The identity of protein was annotated using the SwissProt database (542782 sequences; 193019802 residues). To achieve the best possible results search parameters were as follows: one miscleavage was set for trypsin specificity, carbamidomethyl modification of cysteine and oxidation of methionine were selected as fixed and optional modifications, respectively. At a mass tolerance of 5 ppm, only protein scores greater than 70 ($p < 0.05$) were assigned significant with an expect value 10^{-7}.

Protein extraction and enzymatic assays

Apoplastic washes were obtained from mature leaves of 4 week-old *Arabidopsis* plants by vacuum-infiltrating complete rosettes with 20 mM sodium acetate, pH 5.2. Afterwards, leaf tissue was dipped dry on paper towels, placed in 50 ml Falcon tubes and spun at 1000 g for 5 min at 4°C. Collected fluids were 10-fold concentrated using Vivaspin 500 columns with a 3 kDa cut-off (GE Healthcare).

.Isolation of mesophyll protoplasts from leaves of 4-5 week-old *Arabidopsis* plants was performed according to a protocol described (Yoo et al., 2007). Isolated protoplasts were resuspended in W5 solution (2 mM MES, pH 5.7, 154 mM NaCl, 125 mM $CaCl_2$, 5 mM KCl) and incubated overnight at RT

525 in the dark ($2x10^5$ protoplasts in 1 ml W5 solution). Subsequently, protoplasts were removed by
526 centrifugation (20 sec, 800 rpm, 4°C) and secreted proteins in the medium were concentrated using
527 Vivaspin 2 columns with a 10 kDa cut-off (GE Healthcare).
528 Total protein extracts from the harvested protoplast pellet or 4-5 week-old leaves of *A. thaliana* or *N.*
529 *benthamiana* were prepared using 20 mM sodium acetate, pH 5.2 supplemented with15 mM β-
530 Mercaptoethanol and proteinase inhibitor cocktail (Roche Applied Science, Mannheim, Germany).
531 Approximately 40-60 µg total protein of the leaf extracts or 15 µg of the protoplast samples were
532 added to the enzyme assays. For all in-tube enzyme assays described in the supplemental
533 information, the reaction mix was incubated with shaking at 37°C in 20 mM sodium acetate, pH 5.2.
534 The 4-MUCT chitinase assay was performed as described (Brunner et al., 1998). Briefly, the hydrolytic
535 activity towards 4-methylumbelliferyl-β-D-N, N', N'' triacetylchitotriose (4-MUCT, Sigma-Aldrich) was
536 measured for 30 minutes and compared with that of 2 µg *Streptomyces griseus* chitinase (Sigma-
537 Aldrich). After enzyme incubation in 250 µl final volume of 0.05 % (w/v) 4-MUCT, 20 µl of the reaction
538 mixture were removed and added to 980 µl 0.2 M sodium carbonate solution. Free 4-MU (Sigma-
539 Aldrich) was used for the generation of a standard curve. The intensity of the fluorescence was
540 monitored with an MWG Sirius HT fluorescence microplate reader. For the zymogram, a discontinous
541 CTAB polyacrylamid gel electrophoresis was performed using a 12 % separating gel (43 mM KOH,
542 280 mM acetic acid, pH 4.0, 12% (v/v) acrylamide bisacrylamide 37.5:1, 8% (v/v) glycerol, 1.3%
543 ammonium persulphate and 0.16% TEMED), overlaid by a 4 % stacking gel (64 mM KOH, 94 mM
544 acetic acid, pH 5.1, 4% acrylamide, 1.25% ammonium persulphate and 0.125% TEMED). Prior to
545 loading, the gel was pre-run using anode buffer (40 mM beta-alanine, 70 mM acetic acid, 0.1% CTAB,
546 pH 4.0) and cathode buffer (50 mM KOH, 56 mM acetic acid, pH 5.7, 0.1% CTAB) for 1 hour at 250
547 Volt. Crude protein extracts were mixed with an equal volume of loading buffer (5 M urea, 25 mM KAc
548 pH 6.8, methylene blue) and separated for 2 hours at 150 Volt and 4°C. After electrophoresis, the
549 CTAB-gel was washed with 20 mM NaAc, then sprayed with 0.00625 % (w/v) 4-MUCT in 20 mM
550 NaAc, pH 5.2 and incubated at 37°C for 30 minutes. Fluorescent bands were documented under UV
551 light using the Infinity-3026WL/26MX gel imaging system (PeqLab, Erlangen, Germany).
552 The turbidity assay was done as described previously (Park et al., 2002). Lytic activity towards
553 *Micrococcus luteus* cell wall preparations or *B. subtilis* peptidoglycan (Invivogen, Cecolabs) was
554 measured for 4 hours and compared with that of 1 µg hen egg white lysozyme (Sigma-Aldrich). 1 ml
555 0.02 % (w/v) *M. luteus* cells or PGN suspension was incubated together with the enzyme and the

556 decrease in absorbance at 570 nm of the suspension was measured with a spectrophotometer over
557 time.
558 The 4-MUC cellulase assay was performed using 4-methylumbelliferyl-β-D-cellobioside (4-MUC,
559 Sigma-Aldrich) as substrate. 1 mM 4-MUC was incubated in 20 mM sodium acetate (pH 5.2) at 37°C
560 for 1 hour in a 96 well plate with either 40 µg purified LYS1 or cellulase (Duchefa, Haarlem, The
561 Netherlands) in a total volume of 100 µl. The reaction was stopped with 0.2 M Na_2CO_3 and the
562 intensity of the fluorescence was monitored with an MWG Sirius HT fluorescence microplate reader
563 using excitation and emission wavelengths of 365 nm and 455 nm, respectively.
564
565 **HPLC-analysis**
566 500 µg/ml *B. subtilis* PGN was incubated with 140 µg LYS1 purified from *LYS1*^{OE} plants or controls in
567 20 mM sodium acetate, pH 5.2, at 37°C with shaking for 7 hours. After stopping the reaction by
568 heating at 100°C for 10 minutes, the reaction was centrifuged and the supernatant analyzed by HPLC.
569 The analyses were done by Cecolabs on an Agilent 1200 system with a Prontosil C18-RP column
570 (Bischoff Chromatography, Leonberg, Germany). The mobile phase was (A) 100 mM sodium
571 phosphate, 5 % (v/v) methanol and (B) 100 mM sodium phosphate, 30 % (v/v) methanol.
572
573 **Immune responses**
574 RNA isolation, semi-quantitative RT-PCR and RT-qPCR analysis were performed as described
575 previously (Willmann et al., 2011, Kemmerling et al., 2007). For RT-qPCR, all quantifications were
576 made in duplicate on RNA samples obtained from three independent experiments, each performed
577 with a pool of 3-5 seedlings or two leaves. *EF1a* transcripts served normalization; corresponding water
578 controls were set to 1. The sequences of the primers used for PCR amplifications are given in Table 1.
579 The histochemical detection of ß-glucuronidase (GUS) enzyme activity in whole leaves of
580 *pLYS1::GUS* or *pPR-1::GUS* transgenic *Arabidopsis* (Shapiro and Zhang, 2001) was determined as
581 described earlier (Gust et al., 2007). For the measurement of extracellular pH, 300 µl of cultured rice
582 cells were transferred to 48 well-plates and equilibrated at 150 rpm for 30 min. After addition of
583 elicitors the pH in the cell culture was monitored with an InLab® Micro electrode (Mettler Toledo,
584 Gießen, Germany).
585 For assays with LYS1-digested PGN, 100 µg/ml *B. subtilis* PGN was incubated with 40 µg LYS1
586 purified from *LYS1*^{OE} plants or controls in 2.5 mM MES, pH 5.2, at 37°C with shaking for 4 hours. After

stopping the reaction by heating at 100°C for 10 minutes, the reaction was centrifuged and the supernatant used for triggering immune responses.

Statistical Methods

Statistical significance between two groups has been checked by using Student's t-test. Asterisks represent significant differences (*$p < 0.05$; **$p < 0.01$; ***$p < 0.001$). One-way analysis of variance (ANOVA) was performed for multiple comparisons combined with Duncan's multiple range test indicating significant differences with different letters ($p < 0.05$).

Acknowledgements

We thank Andreas Kulik and Friedrich Götz for bacteria fermentation and Gary Stacey and Michel Legrand for providing the anti-CERK1 and anti-class III chitinase antibody, respectively.

References

AMIN, B., MAURER, A., VOELTER, W., MELMS, A. & KALBACHER, H. 2014. New poteintial serum biomarkers in multiple sclerosis identified by proteomic strategies. *Curr Med Chem,* 21**,** 1544-56.

AUDY, P., BENHAMOU, N., TRUDEL, J. & ASSELIN, A. 1988. Immunocytochemical localization of a wheat germ lysozyme in wheat embryo and coleoptile cells and cytochemical study of its interaction with the cell wall. *Plant Physiol,* 88**,** 1317-22.

BEINTEMA, J. J., JEKEL, P. A. & HARTMANN, J. B. H. 1991. The Primary Structure of Hevamine, an Enzyme with Lysozyme/Chitinase Activity from *Hevea brasiliensis* latex. *European Journal of Biochemistry,* 200**,** 123-130.

BISCHOFF, V., VIGNAL, C., DUVIC, B., BONECA, I. G., HOFFMANN, J. A. & ROYET, J. 2006. Downregulation of the Drosophila Immune Response by Peptidoglycan-Recognition Proteins SC1 and SC2. *PLoS Pathog.,* 2**,** e14.

BOKMA, E., VAN KONINGSVELD, G. A., JERONIMUS-STRATINGH, M. & BEINTEMA, J. J. 1997. Hevamine, a chitinase from the rubber tree Hevea brasiliensis, cleaves peptidoglycan between the C-1 of N-acetylglucosamine and C-4 of N-acetylmuramic acid and therefore is not a lysozyme. *FEBS Lett,* 411**,** 161-3.

BOLLER, T. & FELIX, G. 2009. A renaissance of elicitors: perception of microbe-associated molecular patterns and danger signals by pattern-recognition receptors. *Annu Rev Plant Biol,* 60**,** 379-406.

BOLTE, S., TALBOT, C., BOUTTE, Y., CATRICE, O., READ, N. D. & SATIAT-JEUNEMAITRE, B. 2004. FM-dyes as experimental probes for dissecting vesicle trafficking in living plant cells. *J Microsc,* 214**,** 159-73.

BORCHERT, N., DIETERICH, C., KRUG, K., SCHUTZ, W., JUNG, S., NORDHEIM, A., SOMMER, R. J. & MACEK, B. 2010. Proteogenomics of Pristionchus pacificus reveals distinct proteome structure of nematode models. *Genome Res,* 20**,** 837-46.

BOUDREAU, M. A., FISHER, J. F. & MOBASHERY, S. 2012. Messenger functions of the bacterial cell wall-derived muropeptides. *Biochemistry,* 51**,** 2974-90.

BROCK, A. K., WILLMANN, R., KOLB, D., GREFEN, L., LAJUNEN, H. M., BETHKE, G., LEE, J., NURNBERGER, T. & GUST, A. A. 2010. The Arabidopsis mitogen-activated protein kinase phosphatase PP2C5 affects seed germination, stomatal aperture, and abscisic acid-inducible gene expression. *Plant Physiol,* 153**,** 1098-111.

BROZ, P. & MONACK, D. M. 2013. Newly described pattern recognition receptors team up against intracellular pathogens. *Nat Rev Immunol,* 13**,** 551-65.

BRUNNER, F., STINTZI, A., FRITIG, B. & LEGRAND, M. 1998. Substrate specificities of tobacco chitinases. *Plant J,* 14**,** 225-34.

CALLEWAERT, L. & MICHIELS, C. W. 2010. Lysozymes in the animal kingdom. *J Biosci,* 35**,** 127-60.

CHEONG, J. J., BIRBERG, W., FUGEDI, P., PILOTTI, A., GAREGG, P. J., HONG, N., OGAWA, T. & HAHN, M. G. 1991. Structure-activity relationships of oligo-beta-glucoside elicitors of phytoalexin accumulation in soybean. *Plant Cell,* 3**,** 127-36.

CHISHOLM, S. T., COAKER, G., DAY, B. & STASKAWICZ, B. J. 2006. Host-microbe interactions: shaping the evolution of the plant immune response. *Cell,* 124**,** 803-14.

CHO, J. H., FRASER, I. P., FUKASE, K., KUSUMOTO, S., FUJIMOTO, Y., STAHL, G. L. & EZEKOWITZ, R. A. B. 2005. Human peptidoglycan recognition protein S is an effector of neutrophil-mediated innate immunity. *Blood,* 106**,** 2551-2558.

CLARKE, T. B. & WEISER, J. N. 2011. Intracellular sensors of extracellular bacteria. *Immunol Rev,* 243**,** 9-25.

CLOUGH, S. J. & BENT, A. F. 1998. Floral dip: a simplified method for Agrobacterium-mediated transformation of Arabidopsis thaliana. *Plant J,* 16**,** 735-43.

CONZELMANN, M., WILLIAMS, E. A., KRUG, K., FRANZ-WACHTEL, M., MACEK, B. & JEKELY, G. 2013. The neuropeptide complement of the marine annelid Platynereis dumerilii. *BMC Genomics,* 14**,** 906.

COX, J. & MANN, M. 2008. MaxQuant enables high peptide identification rates, individualized p.p.b.-range mass accuracies and proteome-wide protein quantification. *Nat Biotechnol,* 26**,** 1367-72.

COX, J., NEUHAUSER, N., MICHALSKI, A., SCHELTEMA, R. A., OLSEN, J. V. & MANN, M. 2011. Andromeda: a peptide search engine integrated into the MaxQuant environment. *J Proteome Res,* 10**,** 1794-805.

DAVIS, K. M., NAKAMURA, S. & WEISER, J. N. 2011. Nod2 sensing of lysozyme-digested peptidoglycan promotes macrophage recruitment and clearance of S. pneumoniae colonization in mice. *J Clin Invest,* 121**,** 3666-76.

DE JONGE, R., VAN ESSE, H. P., KOMBRINK, A., SHINYA, T., DESAKI, Y., BOURS, R., VAN DER KROL, S., SHIBUYA, N., JOOSTEN, M. H. & THOMMA, B. P. 2010. Conserved fungal LysM effector Ecp6 prevents chitin-triggered immunity in plants. *Science,* 329**,** 953-5.

DZIARSKI, R. & GUPTA, D. 2005. Peptidoglycan recognition in innate immunity. *J. Endotoxin Res.,* 11**,** 304-10.

DZIARSKI, R. & GUPTA, D. 2010. Mammalian peptidoglycan recognition proteins (PGRPs) in innate immunity. *Innate Immunity,* 16**,** 168-174.

ERBS, G., SILIPO, A., ASLAM, S., DE CASTRO, C., LIPAROTI, V., FLAGIELLO, A., PUCCI, P., LANZETTA, R., PARRILLI, M., MOLINARO, A., NEWMAN, M. A. & COOPER, R. M. 2008. Peptidoglycan and muropeptides from pathogens Agrobacterium and Xanthomonas elicit plant innate immunity: structure and activity. *Chem Biol,* 15**,** 438-48.

FELIX, G., DURAN, J. D., VOLKO, S. & BOLLER, T. 1999. Plants have a sensitive perception system for the most conserved domain of bacterial flagellin. *Plant J,* 18**,** 265-76.

FILIPE, S. R., TOMASZ, A. & LIGOXYGAKIS, P. 2005. Requirements of peptidoglycan structure that allow detection by the Drosophila Toll pathway. *EMBO Rep,* 6**,** 327-33.

FLIEGMANN, J., MITHOFER, A., WANNER, G. & EBEL, J. 2004. An ancient enzyme domain hidden in the putative beta-glucan elicitor receptor of soybean may play an active part in the

perception of pathogen-associated molecular patterns during broad host resistance. *J Biol Chem,* 279**,** 1132-40.

GELIUS, E., PERSSON, C., KARLSSON, J. & STEINER, H. 2003. A mammalian peptidoglycan recognition protein with N-acetylmuramoyl-L-alanine amidase activity. *Biochem Biophys Res Commun,* 306**,** 988-94.

GERSTEL, U., CZAPP, M., BARTELS, J. & SCHRODER, J. M. 2009. Rhamnolipid-induced shedding of flagellin from Pseudomonas aeruginosa provokes hBD-2 and IL-8 response in human keratinocytes. *Cell Microbiol,* 11**,** 842-53.

GLAUNER, B., HOLTJE, J. V. & SCHWARZ, U. 1988. The composition of the murein of Escherichia coli. *J Biol Chem,* 263**,** 10088-95.

GUST, A. A., BISWAS, R., LENZ, H. D., RAUHUT, T., RANF, S., KEMMERLING, B., GOTZ, F., GLAWISCHNIG, E., LEE, J., FELIX, G. & NÜRNBERGER, T. 2007. Bacteria-derived peptidoglycans constitute pathogen-associated molecular patterns triggering innate immunity in Arabidopsis. *J Biol Chem,* 282**,** 32338-48.

HENRISSAT, B. 1991. A classification of glycosyl hydrolases based on amino acid sequence similarities. *Biochem J,* 280 (Pt 2)**,** 309-16.

ISHII, K. J., KOYAMA, S., NAKAGAWA, A., COBAN, C. & AKIRA, S. 2008. Host innate immune receptors and beyond: making sense of microbial infections. *Cell Host Microbe,* 3**,** 352-63.

JANEWAY, C. A., JR. & MEDZHITOV, R. 2002. Innate immune recognition. *Annu Rev Immunol,* 20**,** 197-216.

JENAL, U. & STEPHENS, C. 2002. The Caulobacter cell cycle: timing, spatial organization and checkpoints. *Curr Opin Microbiol,* 5**,** 558-63.

JOHNSON, J. W., FISHER, J. F. & MOBASHERY, S. 2013. Bacterial cell-wall recycling. *Ann N Y Acad Sci,* 1277**,** 54-75.

JONES, J. D. & DANGL, J. L. 2006. The plant immune system. *Nature,* 444**,** 323-9.

KÄLL, L., STOREY, J. D., MACCOSS, M. J. & NOBLE, W. S. 2008. Posterior error probabilities and false discovery rates: two sides of the same coin. *J Proteome Res,* 7**,** 40-4.

KARIMI, M., DE MEYER, B. & HILSON, P. 2005. Modular cloning in plant cells. *Trends Plant Sci,* 10**,** 103-5.

KARIMI, M., INZE, D. & DEPICKER, A. 2002. GATEWAY vectors for Agrobacterium-mediated plant transformation. *Trends Plant Sci,* 7**,** 193-5.

KEMMERLING, B., SCHWEDT, A., RODRIGUEZ, P., MAZZOTTA, S., FRANK, M., QAMAR, S. A., MENGISTE, T., BETSUYAKU, S., PARKER, J. E., MUSSIG, C., THOMMA, B. P., ALBRECHT, C., DE VRIES, S. C., HIRT, H. & NURNBERGER, T. 2007. The BRI1-associated kinase 1, BAK1, has a brassinolide-independent role in plant cell-death control. *Curr Biol,* 17**,** 1116-22.

KROON, L. P. N. M., BROUWER, H., DE COCK, A. W. A. M. & GOVERS, F. 2011. The Genus Phytophthora Anno 2012. *Phytopathology,* 102**,** 348-364.

KUMAR, S., INGLE, H., PRASAD, D. V. & KUMAR, H. 2013. Recognition of bacterial infection by innate immune sensors. *Crit Rev Microbiol,* 39**,** 229-46.

KURATA, S. 2010. Extracellular and intracellular pathogen recognition by Drosophila PGRP-LE and PGRP-LC. *International Immunology,* 22**,** 143-148.

KURATA, S. 2014. Peptidoglycan recognition proteins in Drosophila immunity. *Dev Comp Immunol,* 42**,** 36-41.

KWON, H. K., YOKOYAMA, R. & NISHITANI, K. 2005. A proteomic approach to apoplastic proteins involved in cell wall regeneration in protoplasts of Arabidopsis suspension-cultured cells. *Plant Cell Physiol,* 46**,** 843-57.

LIN, N. C. & MARTIN, G. B. 2005. An avrPto/avrPtoB mutant of Pseudomonas syringae pv. tomato DC3000 does not elicit Pto-mediated resistance and is less virulent on tomato. *Mol Plant Microbe Interact,* 18**,** 43-51.

LIU, B., LI, J. F., AO, Y., QU, J., LI, Z., SU, J., ZHANG, Y., LIU, J., FENG, D., QI, K., HE, Y., WANG, J. & WANG, H. B. 2012a. Lysin motif-containing proteins LYP4 and LYP6 play dual roles in peptidoglycan and chitin perception in rice innate immunity. *Plant Cell,* 24**,** 3406-19.

LIU, T., LIU, Z., SONG, C., HU, Y., HAN, Z., SHE, J., FAN, F., WANG, J., JIN, C., CHANG, J., ZHOU, J. M. & CHAI, J. 2012b. Chitin-induced dimerization activates a plant immune receptor. *Science,* 336**,** 1160-4.

MAGALHAES, J. G., SORBARA, M. T., GIRARDIN, S. E. & PHILPOTT, D. J. 2011. What is new with Nods? *Curr Opin Immunol,* 23**,** 29-34.

MAURER, A., ZEYHER, C., AMIN, B. & KALBACHER, H. 2013. A periodate-cleavable linker for functional proteomics under slightly acidic conditions: application for the analysis of intracellular aspartic proteases. *J Proteome Res,* 12**,** 199-207.

MITHÖFER, A., FLIEGMANN, J., NEUHAUS-URL, G., SCHWARZ, H. & EBEL, J. 2000. The hepta-beta-glucoside elicitor-binding proteins from legumes represent a putative receptor family. *Biol Chem,* 381**,** 705-13.

MONAGHAN, J. & ZIPFEL, C. 2012. Plant pattern recognition receptor complexes at the plasma membrane. *Curr Opin Plant Biol,* 15**,** 349-57.

MÜLLER-ANSTETT, M. A., MÜLLER, P., ALBRECHT, T., NEGA, M., WAGENER, J., GAO, Q., KAESLER, S., SCHALLER, M., BIEDERMANN, T. & GÖTZ, F. 2010. Staphylococcal peptidoglycan co-localizes with Nod2 and TLR2 and activates innate immune response via both receptors in primary murine keratinocytes. *PLoS One,* 5**,** e13153.

NAKAGAWA, T., KUROSE, T., HINO, T., TANAKA, K., KAWAMUKAI, M., NIWA, Y., TOYOOKA, K., MATSUOKA, K., JINBO, T. & KIMURA, T. 2007. Development of series of gateway binary vectors, pGWBs, for realizing efficient construction of fusion genes for plant transformation. *J Biosci Bioeng,* 104**,** 34-41.

NEWMAN, M. A., SUNDELIN, T., NIELSEN, J. T. & ERBS, G. 2013. MAMP (microbe-associated molecular pattern) triggered immunity in plants. *Front Plant Sci,* 4**,** 139.

NIGRO, G., FAZIO, L. L., MARTINO, M. C., ROSSI, G., TATTOLI, I., LIPAROTI, V., DE CASTRO, C., MOLINARO, A., PHILPOTT, D. J. & BERNARDINI, M. L. 2008. Muramylpeptide shedding modulates cell sensing of Shigella flexneri. *Cell Microbiol,* 10**,** 682-95.

NÜRNBERGER, T., BRUNNER, F., KEMMERLING, B. & PIATER, L. 2004. Innate immunity in plants and animals: striking similarities and obvious differences. *Immunol Rev,* 198**,** 249-66.

PARK, J. T. & UEHARA, T. 2008. How bacteria consume their own exoskeletons (turnover and recycling of cell wall peptidoglycan). *Microbiol Mol Biol Rev,* 72**,** 211-27, table of contents.

PARK, S. M., KIM, D. H., TRUONG, N. H. & ITOH, Y. 2002. Heterologous expression and characterization of class III chitinases from rice (*Oryza sativa* L.) *Enzyme and Microbial Technology,* 30**,** 697-702.

PASSARINHO, P. A. & DE VRIES, S. C. 2002. Arabidopsis Chitinases: a Genomic Survey. *The Arabidopsis Book***,** e0023.

PEL, M. J. & PIETERSE, C. M. 2013. Microbial recognition and evasion of host immunity. *J Exp Bot,* 64**,** 1237-48.

POSTEL, S., KUFNER, I., BEUTER, C., MAZZOTTA, S., SCHWEDT, A., BORLOTTI, A., HALTER, T., KEMMERLING, B. & NÜRNBERGER, T. 2010. The multifunctional leucine-rich repeat

receptor kinase BAK1 is implicated in Arabidopsis development and immunity. *Eur J Cell Biol,* 89**,** 169-74.

RAMOS, H. C., RUMBO, M. & SIRARD, J. C. 2004. Bacterial flagellins: mediators of pathogenicity and host immune responses in mucosa. *Trends Microbiol,* 12**,** 509-17.

REITH, J. & MAYER, C. 2011. Peptidoglycan turnover and recycling in Gram-positive bacteria. *Appl Microbiol Biotechnol,* 92**,** 1-11.

ROYET, J. & DZIARSKI, R. 2007. Peptidoglycan recognition proteins: pleiotropic sensors and effectors of antimicrobial defences. *Nat Rev Microbiol,* 5**,** 264-77.

SAKTHIVEL, M., KARTHIKEYAN, N. & PALANI, P. 2010. Detection and analysis of lysozyme activity in some tuberous plants and Calotropis procera's latex. *Journal of Phytology,* 2**,** 65-72.

SCHLEIFER, K. H. & KANDLER, O. 1972. Peptidoglycan types of bacterial cell walls and their taxonomic implications. *Bacteriol Rev,* 36**,** 407-77.

SCHULTE, A., LORENZEN, I., BOTTCHER, M. & PLIETH, C. 2006. A novel fluorescent pH probe for expression in plants. *Plant Methods,* 2**,** 7.

SCHWAB, R., OSSOWSKI, S., RIESTER, M., WARTHMANN, N. & WEIGEL, D. 2006. Highly specific gene silencing by artificial microRNAs in Arabidopsis. *Plant Cell,* 18**,** 1121-1133.

SCHWAB, R., PALATNIK, J. F., RIESTER, M., SCHOMMER, C., SCHMID, M. & WEIGEL, D. 2005. Specific effects of microRNAs on the plant transcriptome. *Dev Cell,* 8**,** 517-27.

SEGONZAC, C. & ZIPFEL, C. 2011. Activation of plant pattern-recognition receptors by bacteria. *Curr Opin Microbiol,* 14**,** 54-61.

SHAPIRO, A. D. & ZHANG, C. 2001. The role of NDR1 in avirulence gene-directed signaling and control of programmed cell death in Arabidopsis. *Plant Physiol,* 127**,** 1089-101.

SMITH, K. D., ANDERSEN-NISSEN, E., HAYASHI, F., STROBE, K., BERGMAN, M. A., BARRETT, S. L., COOKSON, B. T. & ADEREM, A. 2003. Toll-like receptor 5 recognizes a conserved site on flagellin required for protofilament formation and bacterial motility. *Nat Immunol,* 4**,** 1247-53.

SORBARA, M. T. & PHILPOTT, D. J. 2011. Peptidoglycan: a critical activator of the mammalian immune system during infection and homeostasis. *Immunol Rev,* 243**,** 40-60.

STROBER, W., MURRAY, P. J., KITANI, A. & WATANABE, T. 2006. Signalling pathways and molecular interactions of NOD1 and NOD2. *Nat Rev Immunol,* 6**,** 9-20.

800 STUART, L. M., PAQUETTE, N. & BOYER, L. 2013. Effector-triggered versus pattern-triggered
801 immunity: how animals sense pathogens. *Nat Rev Immunol,* 13**,** 199-206.
802 SUN, Y., LI, L., MACHO, A. P., HAN, Z., HU, Z., ZIPFEL, C., ZHOU, J. M. & CHAI, J. 2013. Structural
803 basis for flg22-induced activation of the Arabidopsis FLS2-BAK1 immune complex. *Science,*
804 342**,** 624-8.
805 TEH, O. K. & MOORE, I. 2007. An ARF-GEF acting at the Golgi and in selective endocytosis in
806 polarized plant cells. *Nature,* 448**,** 493-6.
807 VAN LOON, L. C., REP, M. & PIETERSE, C. M. 2006. Significance of inducible defense-related
808 proteins in infected plants. *Annu Rev Phytopathol,* 44**,** 135-62.
809 VANCE, R. E., ISBERG, R. R. & PORTNOY, D. A. 2009. Patterns of pathogenesis: discrimination of
810 pathogenic and nonpathogenic microbes by the innate immune system. *Cell Host Microbe,* 6**,**
811 10-21.
812 WANG, L., WEBER, A. N., ATILANO, M. L., FILIPE, S. R., GAY, N. J. & LIGOXYGAKIS, P. 2006.
813 Sensing of Gram-positive bacteria in Drosophila: GNBP1 is needed to process and present
814 peptidoglycan to PGRP-SA. *Embo J,* 25**,** 5005-14.
815 WANG, Z. M., LI, X., COCKLIN, R. R., WANG, M., FUKASE, K., INAMURA, S., KUSUMOTO, S.,
816 GUPTA, D. & DZIARSKI, R. 2003. Human peptidoglycan recognition protein-L is an N-
817 acetylmuramoyl-L-alanine amidase. *J Biol Chem,* 278**,** 49044-52.
818 WILLMANN, R., LAJUNEN, H. M., ERBS, G., NEWMAN, M. A., KOLB, D., TSUDA, K., KATAGIRI, F.,
819 FLIEGMANN, J., BONO, J. J., CULLIMORE, J. V., JEHLE, A. K., GOTZ, F., KULIK, A.,
820 MOLINARO, A., LIPKA, V., GUST, A. A. & NÜRNBERGER, T. 2011. Arabidopsis lysin-motif
821 proteins LYM1 LYM3 CERK1 mediate bacterial peptidoglycan sensing and immunity to
822 bacterial infection. *Proc Natl Acad Sci U S A,* 108**,** 19824-9.
823 WILLMANN, R. & NÜRNBERGER, T. 2012. How plant lysin motif receptors get activated: lessons
824 learned from structural biology. *Sci Signal,* 5**,** pe28.
825 WYCKOFF, T. J., TAYLOR, J. A. & SALAMA, N. R. 2012. Beyond growth: novel functions for bacterial
826 cell wall hydrolases. *Trends Microbiol,* 20**,** 540-7.
827 YOKOGAWA, K., KAWATA, S., TAKEMURA, T. & YOSHIMURA, Y. 1975. Purification and properties
828 of lytic enzymes from *Streptomyces globisporus* 1829. *Agric Biol Chem,* 39**,** 1533-1543.
829 YOO, S. D., CHO, Y. H. & SHEEN, J. 2007. Arabidopsis mesophyll protoplasts: a versatile cell system
830 for transient gene expression analysis. *Nat Protoc,* 2**,** 1565-72.

ZHANG, B., RAMONELL, K., SOMERVILLE, S. & STACEY, G. 2002. Characterization of early, chitin-induced gene expression in Arabidopsis. *Mol Plant Microbe Interact,* 15**,** 963-70.

Figure titles and legends

Figure 1. The Arabidopsis *lysozyme 1 (LYS1)* gene is transcriptionally activated upon pathogen-infection

(**A**) LYM1 and LYM3 do not possess PGN-hydrolytic activity. *M. luteus* cell wall preparations were incubated with 20 µg of affinity-purified His6-tagged LYM1 or LYM3 or 0.5 µg hen egg-white lysozyme and PGN-hydrolytic activity was assayed in a turbidity assay at indicated time points. As negative control (nc) non-induced His6-tagged LYM3 bacterial lysates were used for affinity purification and eluates were subjected to turbidity assays. Means ± S.D. of three replicates per sample are given. Statistical significance compared to the negative control (** $p < 0.001$, *** $p < 0.0001$, Student's t-test) is indicated by asterisks. (**B**) Multiple sequence alignment of the 24 Arabidopsis chitinases using the ClustalW2 algorithm. Full length amino acid sequences were aligned and subgroups were classified according to Passarinho and de Vries (2002). Arabidopsis *lysozyme 1* (*LYS1, At5g24090*) represents the only member of class III. (**C**) The expression of *LYS1* in transgenic *pLYS1::GUS* reporter plants. Leaf halves of transgenic *pLYS1::GUS* or *pPR1::GUS* reporter plants were infiltrated with the virulent *Pseudomonas syringae* pv. *tomato* (*Pto*) DC3000, the type III secretion system-deficient *Pto* DC3000 hrcC- or the avirulent *Pseudomonas syringae* pv. *phaseolicola* (*Pph*) strain (10^8 cfu/ml) or 10 mM $MgCl_2$ as control. After 24 h leaves were harvested and stained for GUS activity. (**D**) Leaves of wild type plants were treated for 3 or 24 hours with 1 µM flg22, 100 µg/ml PGN from *Pto* or 100 µg/ml LPS. Total RNA was subjected to RT-PCR using *LYS1* or *FRK1* specific primers. *EF1α* transcript was used for normalization. All experiments shown in panels (A), (C) and (D) were repeated once with similar results.

Figure 2. Analysis of *LYS1* overexpression lines.

(**A)** RT-qPCR analyses of transcript levels in mature leaves of each two independent transgenic lines expressing *p35S::LYS1-GFP* (*$LYS1^{OE}$-1, $LYS1^{OE}$-2*) relative to expression levels in wild type. *EF1a* transcript was used for normalization. Error bars, S.D. (n = 3). Statistical significance compared to wild-type (*** $p < 0.001$, Student's t-test) is indicated by asterisks. (**B**) Immunoblot analysis of protein extracts from leaves of two independent *$LYS1^{OE}$* lines, a LYS1-knock down line (*$LYS1^{KD}$*-1, see Figure

3) and wild type plants. Total leaf protein was separated by SDS-PAGE and blotted onto a nitrocellulose membrane. The immunodetection was carried out using α-tobacco class III chitinase (α-Chit) or α-GFP (both from rabbit) and an anti-rabbit HRP-coupled secondary antibody. Ponceau S red staining of the large subunit of RuBisCO served as loading control. (**C**) Total Protein extracts from leaves of *LYS1*^{OE}*-1* plants were subjected to deglycosylation with a deglycosylation kit (NEB). The negative control (-) was treated as the deglycosylation sample (+) but without addition of the deglycosylation enzyme mix. The immunoblot analysis was carried out as described in (**B**). All experiments shown were repeated at least once.

Figure 3. Analysis of *LYS1* amiRNA lines

(**A**) Predicted LYS1 gene structure (exons, black bars; introns, black lines; untranslated regions, grey). The region targeted by the amiRNA construct is indicated by an arrowhead. **(B)** Off-target genes for the *LYS1-amiRNA* construct were identified using the Web microRNA Designer (WMD; http://wmd.weigelworld.org). The region targeted by the amiRNA is given for each gene, mismatches are indicated in red. Potential off targets either possess more than one mismatch at positions 2-12 or have mismatches at position 10 and/or 11 which will limit amiRNA function. **(C)** Transcript levels of the four top hits shown in **(B)** were determined by RT-qPCR in untreated seedlings of two independent transgenic *LYS1*-amiRNA knock-down lines (*LYS1*^{KD}*-1, LYS1*^{KD}*-2*) using gene specific primers for *LYS1 (At5g24090), At4g02540, At1g05615, At5g58780* and *At3g51010*. *EF1α* transcript was used for normalization. Error bars, S.D. (n = 3). Statistical significance compared to the wild type control (which was set to 1 for each primer set) is indicated by asterisks (*** $p < 0.001$, Student's t-test). The experiment was repeated once with similar results.

Figure 3 - Figure supplement 1. Characterization of *LYS1* T-DNA insertion lines

(A) Predicted *LYS1* gene structure (exons, black bars; introns, black lines; untranslated regions, grey). T-DNA insertion sites are indicated by triangles. **(B)** The T-DNA insertion lines (each two samples) and the corresponding wild type accessions were genotyped using following primer combinations: LP_N853931 and RP_N853931 (WT-PCR, *lys1-1*), Wisc-Lba and RP_853931 (Lba-PCR, *lys1-1*), LP_N595362 and RP_N595362 (WT-PCR, *lys1-2*), Salk-Lba and RP_N595362 (Lba-PCR, *lys1-2*), At5g24090F1 and At5g24090R1 (WT-PCR, *lys1-3*) and Ds5-1 and At5g24090R1 (Lba-PCR, *lys1-3*). **(C)** The *LYS1* transcript analysis in mature leaves was done by semi-quantitative RT-PCR using

following primer combinations: At5g24090F and At5g24090R (*lys1-1* and *lys1-2*) and At5g24090F and At5g24090RP2 (*lys1-3*).

Figure 4. LYS1 is a glucan-hydrolase

(**A-D**) Protein extracts from adult wild type or *LYS^{OE}-1* and *LYS^{KD}-1* homozygous lines were assayed for hydrolytic activity towards glycan substrates. Plants expressing secreted GFP (*secGFP*) served to control the effect of external GFP. (**A**) Leaf protein extracts from indicated transgenic plants were assayed for chitinolytic activity using the 4-MUCT substrate. Enzymatic activities 4 hours post treatment were calculated using *Streptomyces griseus* chitinase as positive control (pc). (**B**) Protein extracts from *LYS1^{OE}-1* or *secGFP* plants were separated on a CTAB-polyacrylamid gel and hydrolytic activity was assayed by overlaying the gel with the substrate 4-MUCT. Fluorescent bands are indicative of substrate cleavage. The arrowhead indicates the position of LYS1. (**C, D**) *M. luteus* cells (**C**) or *B. subtilis* PGN (**D**) was subjected to hydrolysis by leaf protein extracts and PGN hydrolytic activity was calculated after 4 hours using hen egg-white lysozyme as positive control (pc). Significant differences compared to the buffer control are indicated by asterisks (* $p < 0.05$; Student's t-test; A, C, D). (**E**) Protoplasts of transgenic lines were pelleted, and protein extracts of the protoplast (PP) pellet or medium supernatant was subjected to the PGN hydrolysis assay as described in (**C**). As controls buffer or protoplast medium (PP medium) was used. Means ± S.D. of two replicates per sample are given, bars with different letters are significantly different based on one-way ANOVA ($p < 0.05$). (**F**) Lysis of *M. luteus* cells was determined in a turbidity assay with *LYS1^{OE}* leaf protein extracts as described in (**C**) at the indicated pH. Means ± S.D. of two replicates per sample are given. All experiments shown were repeated at least once.

Figure 4 - Figure supplement 1. LYS1 is located in the plant apoplast

(**A**) Apoplastic washes were prepared from leaves of wild type Arabidopsis plants or the *LYS1^{OE}-1 and LYS1^{KD}-1* lines. Apoplastic fluids (10-fold concentrated) or total leaf protein extracts were subjected to western blot analysis using antibodies raised against GFP (α-GFP), tobacco class III chitinase (α-chit) or the cytoplasmic kinase MPK3. (**B**) The *p35S::LYS1-GFP* and *p35S::LYS1ΔSP-GFP* constructs were transiently expressed in *Nicotiana benthamiana* leaves using *Agrobacterium tumefaciens*-mediated transformation. GFP fluorescence in the leaf epidermal cells was analysed 3 days post infection. FM4-64 was used to stain the plasma membrane. Argon/krypton laser was used for

excitation of GFP at 488 nm and the 543 nm line of helium/neon laser for the excitation of FM4-64. Detection wavelengths of emitted light were 500 nm to 600 nm (GFP) and 560 nm to 615 nm (FM4-64). All experiments shown were repeated three times.

Figure 4 - Figure supplement 2. LYS1 is devoid of cellulose hydrolytic activity

LYS1 was purified from 5 weeks old *LYS1*^{OE} plants and used for cellulase activity assays. The substrate 4-MUC as incubated for 1 hour with purified LYS1, commercial reference cellulase or buffer as controls. Fluorescence was determined (ex/em= 365 nm/455 nm) after stopping the reaction with 0.2 M Na_2CO_3. Means ± S.D. of three replicates per sample are given. Statistical significance compared to the buffer control (*** $p < 0.001$, Student's t-test) is indicated by asterisks. The experiment was repeated once with the same result.

Figure 5. LYS1 transiently expressed in *N. benthamiana* possesses hydrolytic activity

(**A**) Protein extracts from *N. benthamiana* leaves expressing LYS1 fused to the myc epitope tag under control of the *p35S* promoter were separated on an SDS-polyacrylamid gel and analysed by western blot using antibodies raised against the myc-epitope tag. As control, plants were infiltrated with agrobacteria harboring the p19 suppressor of silencing construct (p19). Protein sizes (kDa) are indicated on the left. (**B**) *N. benthamiana* protein extracts from leaves expressing *LYS1*$_{myc}$ or p19 were separated on a CTAB-polyacrylamid gel and hydrolytic activity was assayed by overlaying the gel with the substrate 4-MUCT. Fluorescent bands are indicative of substrate cleavage. Arrowheads indicate the positions of epitope-tagged LYS1. (**C**) Protein extracts from *N. benthamiana* leaves expressing *LYS1*$_{myc}$ or p19 were assayed for PGN hydrolytic activity in a turbidity assay using *B. subtilis* PGN. Relative activities (2 hours post treatment) were calculated using hen egg-white lysozyme as standard. Statistical significance compared to the untreated control (* $p < 0.05$, Student's t-test) is indicated by asterisks. All experiments shown were repeated at least once.

Figure 6. Purified LYS1 generates immunogenic PGN fragments

LYS1 was purified from 5 weeks old *LYS1*^{OE} plants and used for PGN digestion. (**A**) 500 µg of *Bacillus subtilis* PGN were digested for 7 hours with either mutanolysin (50 µg/ml), native purified LYS1 (140 µg/ml), heat-denatured purified LYS1 (140 µg/ml) or the reaction buffer alone and subjected to HPLC fractionation. Shown are the peak profiles of representative runs. The signal intensity is given in milli

absorbance units (mAU). (**B**) *B. subtilis* PGN was digested for 4 h as described in (**A**) and Arabidopsis wild type seedlings or the indicated mutant lines were treated for 6 h with 25 µl/ml digest supernatant containing solubilized PGN fragments. Total seedling RNA was subjected to RT-qPCR using *Flagellin responsive kinase* (*FRK1*) specific primers. *EF1α* transcript was used for normalization, water treatment served as control and was set to 1. (**C**) Supernatants of digested PGN (25 µl/ml) was added to cultured rice cells and medium alkalinization was determined at 20 min post addition. Treatment with water or MES buffer served as control. All data represent triplicate samples ± S.D., bars with different letters are significantly different based on one-way ANOVA ($p < 0.05$; B, C). (**D**) *B. subtilis* PGN was digested with native purified LYS1 for the indicated times or overnight (o/n), and digest supernatant was used to trigger medium alkalinization in rice cells as described in (**C**). All data represent triplicate samples ± S.D., asterisks indicate significant differences compared to the buffer control (* $p < 0.05$; ** $p < 0.01$; *** $p < 0.001$; Student's t test). All experiments shown were repeated at least once.

Figure 7. *LYS1* lines are not impaired in resistance towards infection with *Botrytis cinerea*

Five week-old plants were infected with the necrotrophic fungus *Botrytis cinerea*. 5 µl spore suspension of 5 x 10^5 spores/ml was drop-inoculated on the one half of the leaf; two leaves per plant were infected. The plants were analysed for symptom development after 2 and 3 days post infection (dpi). (**A**) Trypan blue stain showing visible symptoms after 2 dpi. (**B**) Microscopic analysis of the infection site and fungal hyphae 2 dpi visualised by Trypan blue stain. (**C**) Measurement of the lesion size 3 dpi. Shown are means and standard errors (n=16). No significant differences were observed (Student's t-test). The experiment was repeated once with the same result.

Figure 8. *LYS1* mutation does not impinge on resistance towards *Alternaria brassicicola*

Five week-old plants were infected with the necrotrophic fungus *Alternaria brassicicola*. Six 5 µl droplets of spore suspension of 5 x 10^5 spores/ml were inoculated on the leaf; two leaves per plant were infected. The plants were analysed for symptom development after 7, 11, and 14 days post infection. (**A**) Visible symptoms of four independent leaves after 14 dpi. (**B**) Disease symptoms after 14 dpi visualised by Trypan blue stain. (**C**) Microscopic analysis of the infection site and fungal hyphae 14 dpi visualised by Trypan blue stain. (**D**) Calculation of the disease index 7, 11 and 14 days post

infection. Shown are means and standard errors (n=16). No significant differences were observed (Student's t-test). The experiment was repeated once with the same result.

Figure 9. Manipulation of *LYS1* levels causes hyper-susceptibility towards bacterial infection and loss of PGN-triggered immune responses.

(**A, B**) Transgenic *LYS1* plants are hyper-susceptible to bacterial infection. Growth of *Pto* DC3000 (**A**) or *Pto* DC3000 Δ*AvrPto/AvrPtoB* (**B**) was determined 2 or 4 days post infiltration of 10^4 colony forming units ml^{-1} (cfu/ml). Data represent means ± S.D. of six replicate measurements/genotype/data point. Representative data of at least four independent experiments are shown. (**C**) Transgenic *LYS1* plants are impaired in PGN-induced immune gene expression. Leaves of wild type plants or transgenic *LYS1* plants were treated for 6 hours with 100 µg *B. subtilis* PGN and total RNA was subjected to RT-qPCR using *FRK1* specific primers. *EF1α* transcript was used for normalization. Data represent means ± S.D. of triplicate samples, and shown is the result of one out of three independent experiments. Statistical significance compared to wild-type (* $p < 0.05$, Student's t-test) is indicated by asterisks.

Figure 9 – Figure supplement 1. Impact of weak *LYS1* overexpression

(**A**) Transcript levels of *LYS1* and the PGN receptors *LYM1*, *LYM3* and *CERK1* in the strong *LYS1* overexpressor line, $LYS1^{OE}$-1, compared to the weak overexpressor line $LYS1^{OE}$-3. Total RNA from untreated seedlings (top panel) or mature leaves (bottom panel) was subjected to RT-qPCR using specific primers for *LYS1*, *LYM1*, *LYM3* or *CERK1*. *EF1α* transcript was used for normalization. Data represent means ± S.D. of triplicate samples. For mature leaves, also CERK1 protein levels were determined using an anti-CERK1 antibody (bottom panel, inset). Ponceau S red staining of the large subunit of RuBisCO served as loading control. (**B**) Immunoblot analysis of protein extracts from leaves of two independent $LYS1^{OE}$ lines ($LYS1^{OE}$*-1,* $LYS1^{OE}$*-3*) and wild type plants. Total leaf protein was subjected to Western blot analysis using α-tobacco class III chitinase (α-Chit) or α-GFP (both from rabbit) and an anti-rabbit HRP-coupled secondary antibody. Ponceau S red staining of the large subunit of RuBisCO served as loading control. (**C**) Growth of *Pto* DC3000 was determined 2 days post infiltration of 10^4 colony forming units ml^{-1} (cfu/ml). Data represent means ± S.D. of six replicate measurements/genotype/data point. Statistical significance compared to wild-type (* $p < 0.05$; ** $p < 0.01$, Student's t-test) is indicated by asterisks. All experiments shown were repeated at least once.

Tables

Table 1. Primers used in this study

AGI	Primer name	Sequence 5' → 3'
At5g24090 (LYS1)	At5g24090F1	CCAGAGGTGGCATAGCCATC
	At5g24090R1	CATCTGGTGGGATATAGCCAC
	At5g24090F	ATGACCAACATGACTCTTCG
	At5g24090R	TCACACACTAGCCAATATAG
	At5g24090RP2	TGATGCCACGAGACTGAC
	LP_N853931	TGACGAACCATGATAAATGGG
	RP_N853931	CATAACCTCACACTGTGCTCG
	LP_N595362	TAGTGCATGCATGTTAAACCG
	RP_N595362	AGCTCCTCAATGTCCATTTCC
	Salk-Lba	TGGTTCACGTAGTGGGCCATCG
	Ds5-1	GAAACGGTCGGGAAACTAGCTCTAC
	Wisc-Lba (p745)	AACGTCCGCAATGTGTTATTAAGTTGTC
	At5g24090Fq	CACTTGCACCCATTTTGGC
	At5g24090Rq	CCTCGACCCAATCGAGTA
	At5g24090miR-s	GATTTGACGTAAGCATACCGCCCTCTCTCTTTTGTATTCC
	At5g24090miR-a	GAGGGCGGTATGCTTACGTCAAATCAAAGAGAATCAATGA
	At5g24090miR*s	GAGGACGGTATGCTTTCGTCAATTCACAGGTCGTGATATG
	At5g24090miR*s	GAATTGACGAAAGCATACCGTCCTCTACATATATATTCCT
	At5g24090gatF	AAAAAGCAGGCTACATGACCAACATGACTCTTCG
	At5g24090gatR	AGAAAGCTGGGTACACACTAGCCAATATAGATG
	At5g24090gatR-STOP	AGAAAGCTGGGTATCACACACTAGCCAATATAG
	At5g24090gatF2	AAAAAGCAGGCTATGCCGTAGGCGAGTGTTTC
	At5g24090gatR2	AGAAAGCTGGGTGTTTTTGGTTAAAGATGTTTG
At1g07920/30/40 (EF1α)	Ef1α-100-f	GAGGCAGACTGTTGCAGTCG
	Ef1α-100-r	TCACTTCGCACCCTTCTTGA
At2g19190 (FRK1)	FRK1-F	AAGAGTTTCGAGCAGAGGTTGAC
	FRK1-R	CCAACAAGAGAAGTCAGGTTCGTG
At4g02540	At4g02540-qf1	GTACCACGCCTATCTATT
	At4g02540-qr1	CTCATAGAAGAAACCAGCA
At1g05615	At1g05615-qf1	GGATTCCTATCTCTACCT
	At1g05615-qr1	TTCTTTACCCTCATCAACC
At5g58780	At5g58780-qf1	CTCTCTTCTCTTTTATCTCTCC
	At5g58780-qr1	CTCCTCCACTCCTACCACA
At3g51010	At3g51010-qf1	GCGTCGTGCTTTTATACTG
	At3g51010-qr1	TTCTTCCTCTTCGCCTCT
At1g21880 (LYM1)	Lym1-100-f	TACAACGGTATAGCCAACGGCACT
	Lym1-100-r	GTGGAGCTAGAAGCGGCGCA

At1g77630 (LYM3)	Lym3-100-f	ACTTCGCAGCAGAGTAGCTC
	Lym3-100-r	AGCGGTGCTAATTGTTGCGG
At3g21630 (CERK1)	CERK1-100-f	GGGCAAGGTGGTTTTGGGGCT
	CERK1-100-r	CCGCCAAGAACTGTTTCGATGCC
	attB1	GGGGACAACTTTGTACAAAAAAGCAGGCT
	attB2	GGGGACCACTTTGTAC AAGAAAGCTGGGT

1029

1030 **Figure supplements:**

1031 Figure 3 - Figure supplement 1. Characterization of *LYS1* T-DNA insertion lines

1032 Figure 4 - Figure supplement 1. LYS1 is located in the plant apoplast

1033 Figure 4 - Figure supplement 2. LYS1 is devoid of cellulose hydrolytic activity

1034 Figure 9 – Figure supplement 1. Impact of weak *LYS1* overexpression

1035

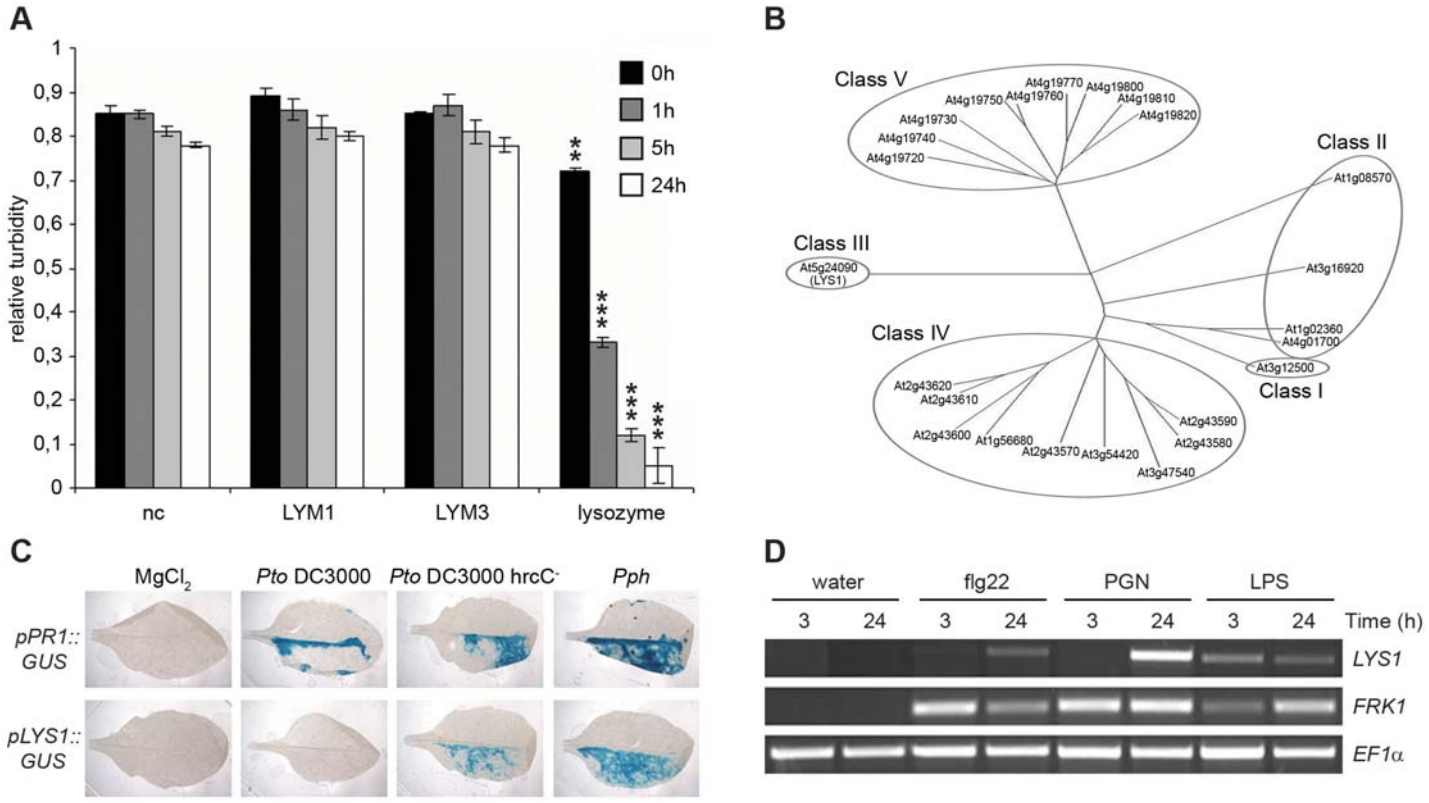
A
relative turbidity
0h
1h
5h
24h
nc
LYM1
LYM3
lysozyme
B
Class V
Class II
Class III
Class IV
Class I
At4g19770
At4g19800
At4g19750
At4g19760
At4g19810
At4g19730
At4g19820
At4g19740
At4g19720
At1g08570
At5g24090 (LYS1)
At3g16920
At1g02360
At4g01700
At3g12500
At2g43620
At2g43610
At2g43590
At2g43600
At1g56680
At2g43580
At2g43570
At3g54420
At3g47540
C
MgCl2
Pto DC3000
Pto DC3000 hrcC-
Pph
pPR1::GUS
pLYS1::GUS
D
water
flg22
PGN
LPS
3
24
Time (h)
LYS1
FRK1
EF1α

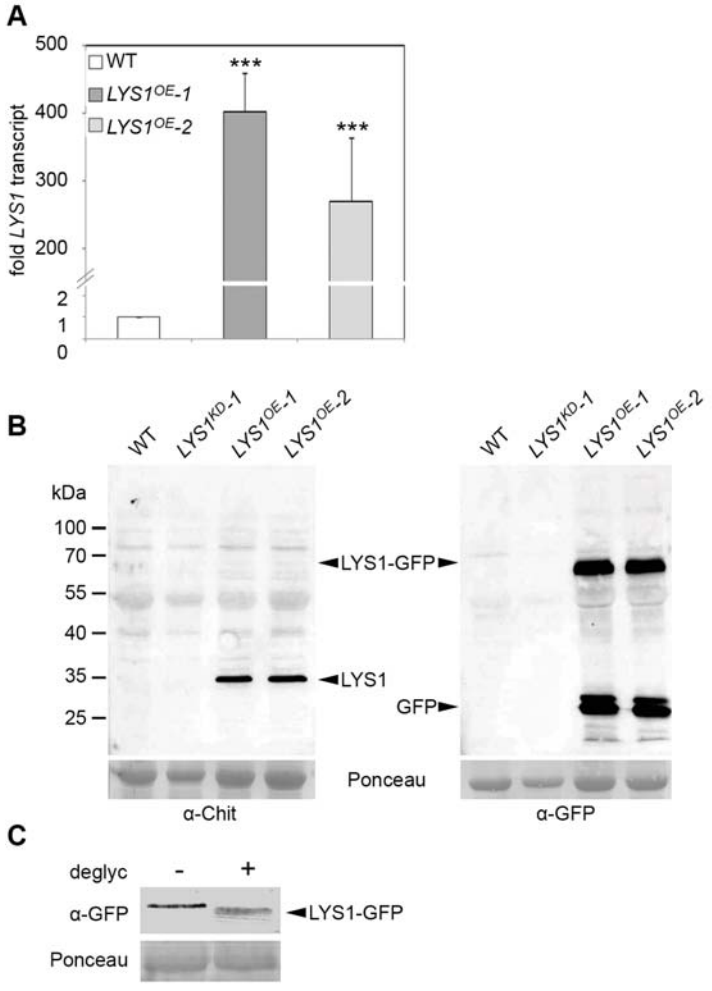
A
500
400
300
200
2
1
0
fold LYS1 transcript
WT
LYS1OE-1
LYS1OE-2
***
***
B
WT
LYS1KD-1
LYS1OE-1
LYS1OE-2
kDa
100
70
55
40
35
25
LYS1-GFP
LYS1
GFP
Ponceau
α-Chit
α-GFP
C
deglyc
-
+
α-GFP
LYS1-GFP
Ponceau

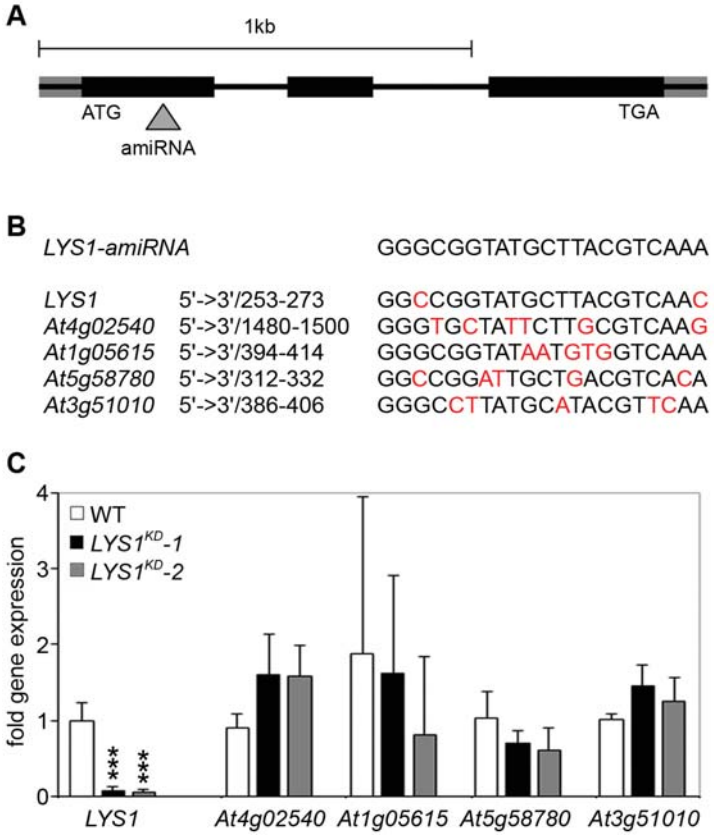
A
1kb
ATG
TGA
amiRNA
B
LYS1-amiRNA GGGCGGTATGCTTACGTCAAA
LYS1 5'->3'/253-273 GGCCGGTATGCTTACGTCAAC
At4g02540 5'->3'/1480-1500 GGGTGCTATTCTTGCGTCAAG
At1g05615 5'->3'/394-414 GGGCGGTATAATGTGGTCAAA
At5g58780 5'->3'/312-332 GGCCGGATTGCTGACGTCACA
At3g51010 5'->3'/386-406 GGGCCTTATGCATACGTTCAA
C
fold gene expression
WT
LYS1KD-1
LYS1KD-2
0
1
2
3
4
***
***
LYS1
At4g02540
At1g05615
At5g58780
At3g51010

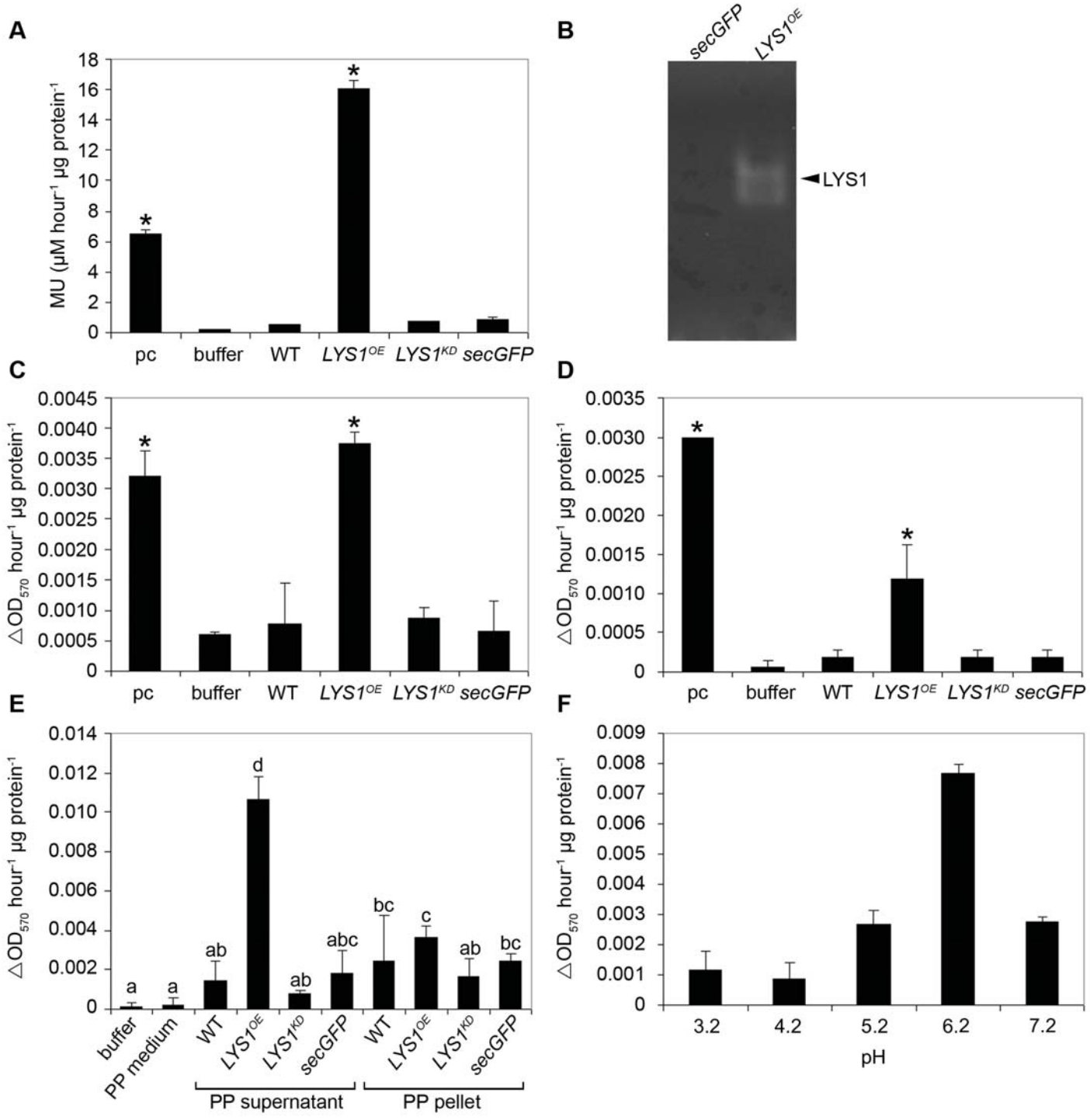
A
MU (μM hour-1 μg protein-1
18
16
14
12
10
8
6
4
2
0
*
*
pc
buffer
WT
LYS1OE
LYS1KD
secGFP
B
secGFP
LYS1OE
LYS1
C
△OD570 hour-1 μg protein-1
0.0045
0.0040
0.0035
0.0030
0.0025
0.0020
0.0015
0.0010
0.0005
0
*
*
pc
buffer
WT
LYS1OE
LYS1KD
secGFP
D
△OD570 hour-1 μg protein-1
0.0035
0.0030
0.0025
0.0020
0.0015
0.0010
0.0005
0
*
*
pc
buffer
WT
LYS1OE
LYS1KD
secGFP
E
△OD570 hour-1 μg protein-1
0.014
0.012
0.010
0.008
0.006
0.004
0.002
0
a
a
ab
d
ab
abc
bc
c
ab
bc
buffer
PP medium
WT
LYS1OE
LYS1KD
secGFP
WT
LYS1OE
LYS1KD
secGFP
PP supernatant
PP pellet
F
△OD570 hour-1 μg protein-1
0.009
0.008
0.007
0.006
0.005
0.004
0.003
0.002
0.001
0
3.2
4.2
5.2
6.2
7.2
pH

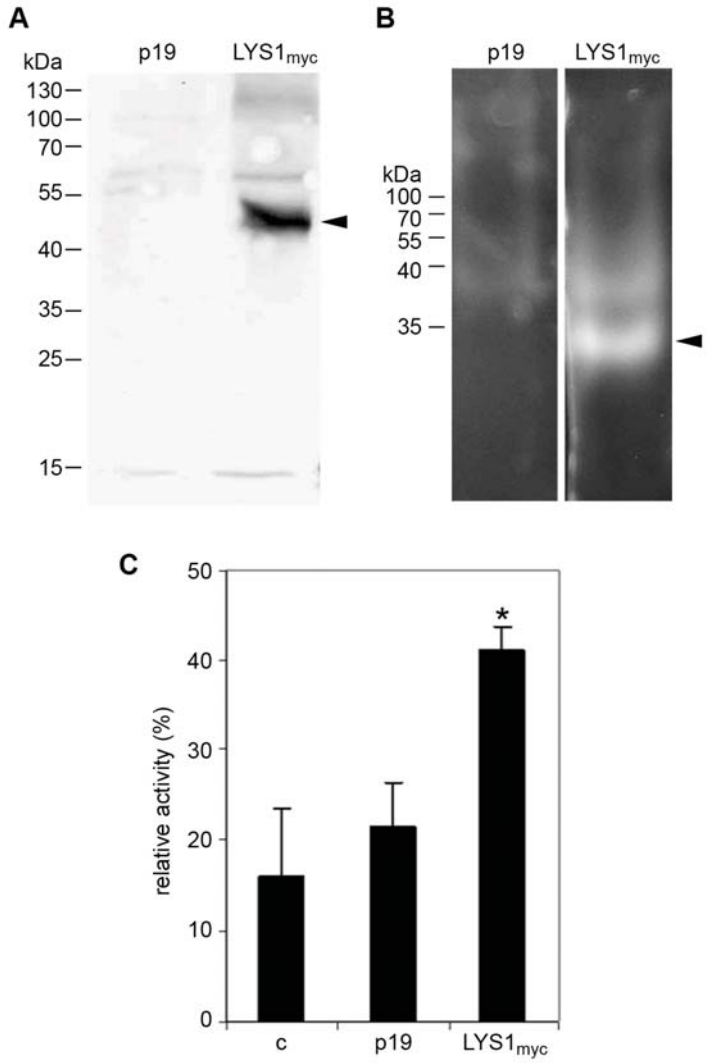
A
p19
LYS1myc
kDa
130
100
70
55
40
35
25
15
B
p19
LYS1myc
kDa
100
70
55
40
35
C
relative activity (%)
50
40
30
20
10
0
*
c
p19
LYS1myc

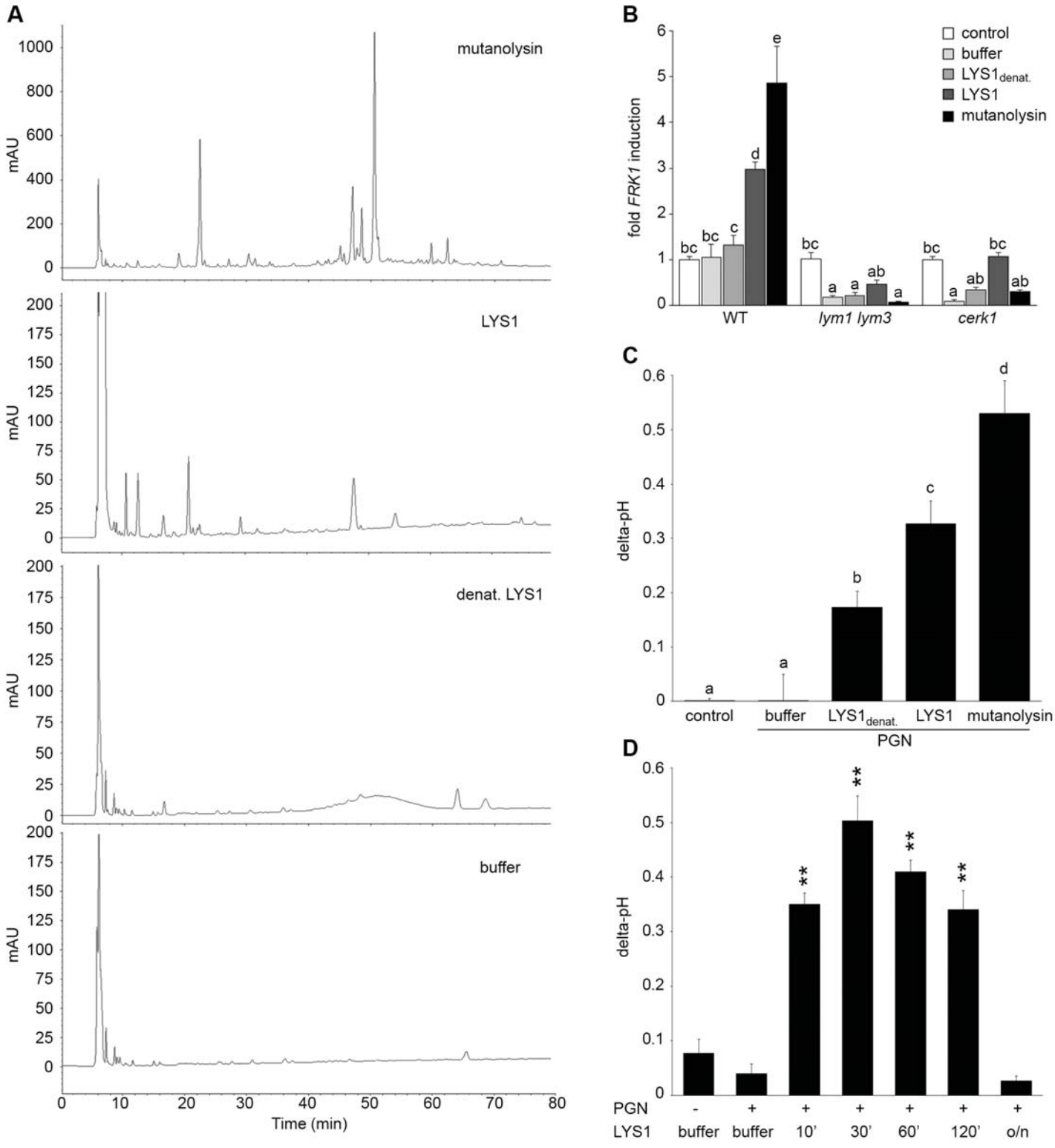
A
mutanolysin
LYS1
denat. LYS1
buffer
mAU
Time (min)
B
control
buffer
LYS1denat.
LYS1
mutanolysin
fold FRK1 induction
WT
lym1 lym3
cerk1
C
delta-pH
control
buffer
LYS1denat.
LYS1
mutanolysin
PGN
D
delta-pH
PGN
LYS1
buffer
10'
30'
60'
120'
o/n

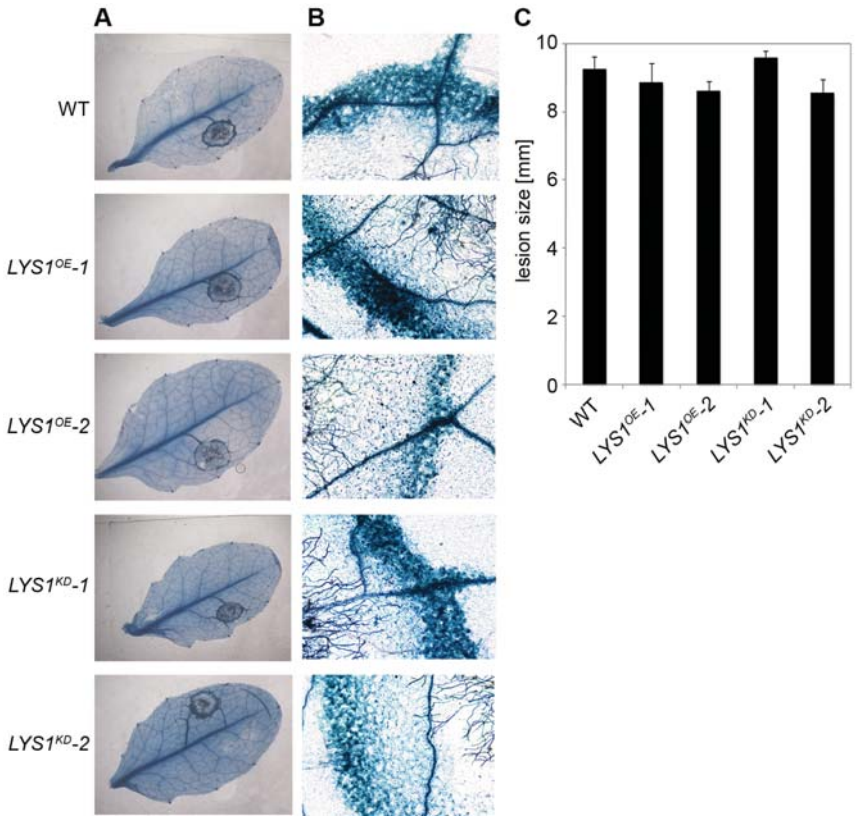
A
B
C
WT
LYS1OE-1
LYS1OE-2
LYS1KD-1
LYS1KD-2
lesion size [mm]
0
2
4
6
8
10
WT
LYS1OE-1
LYS1OE-2
LYS1KD-1
LYS1KD-2

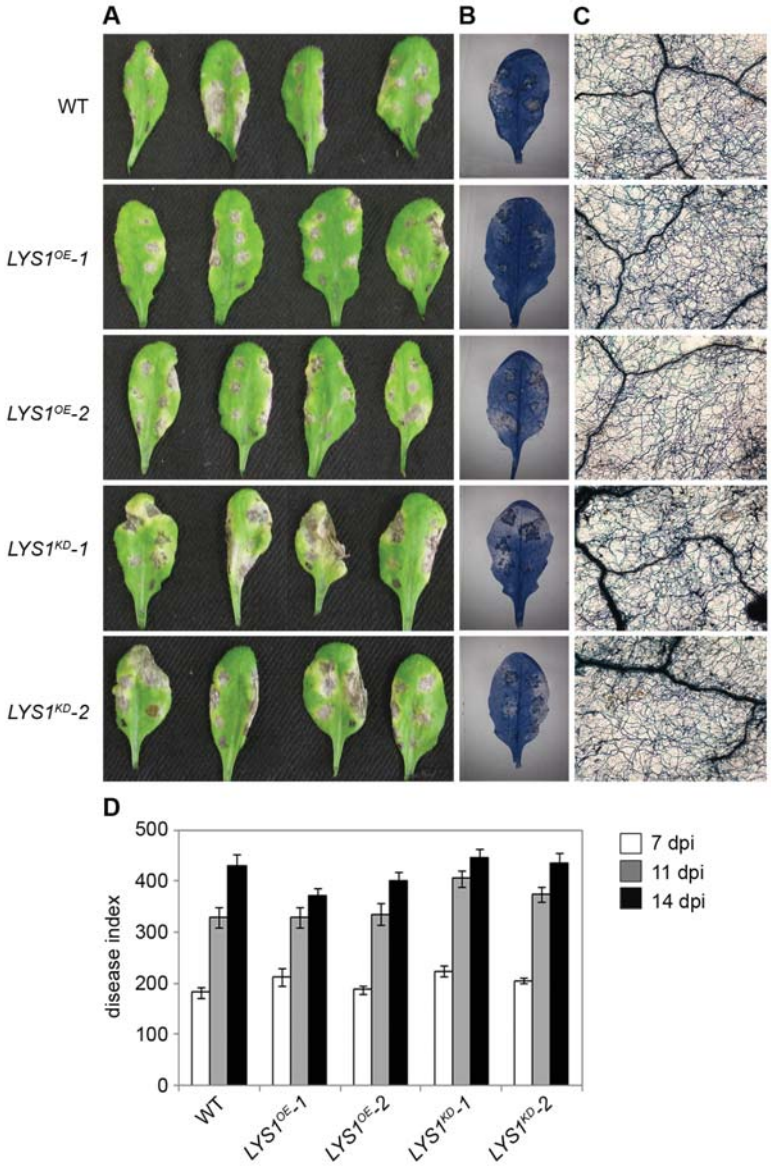
A
B
C
WT
LYS1OE-1
LYS1OE-2
LYS1KD-1
LYS1KD-2
D
disease index
500
400
300
200
100
0
7 dpi
11 dpi
14 dpi
WT
LYS1OE-1
LYS1OE-2
LYS1KD-1
LYS1KD-2

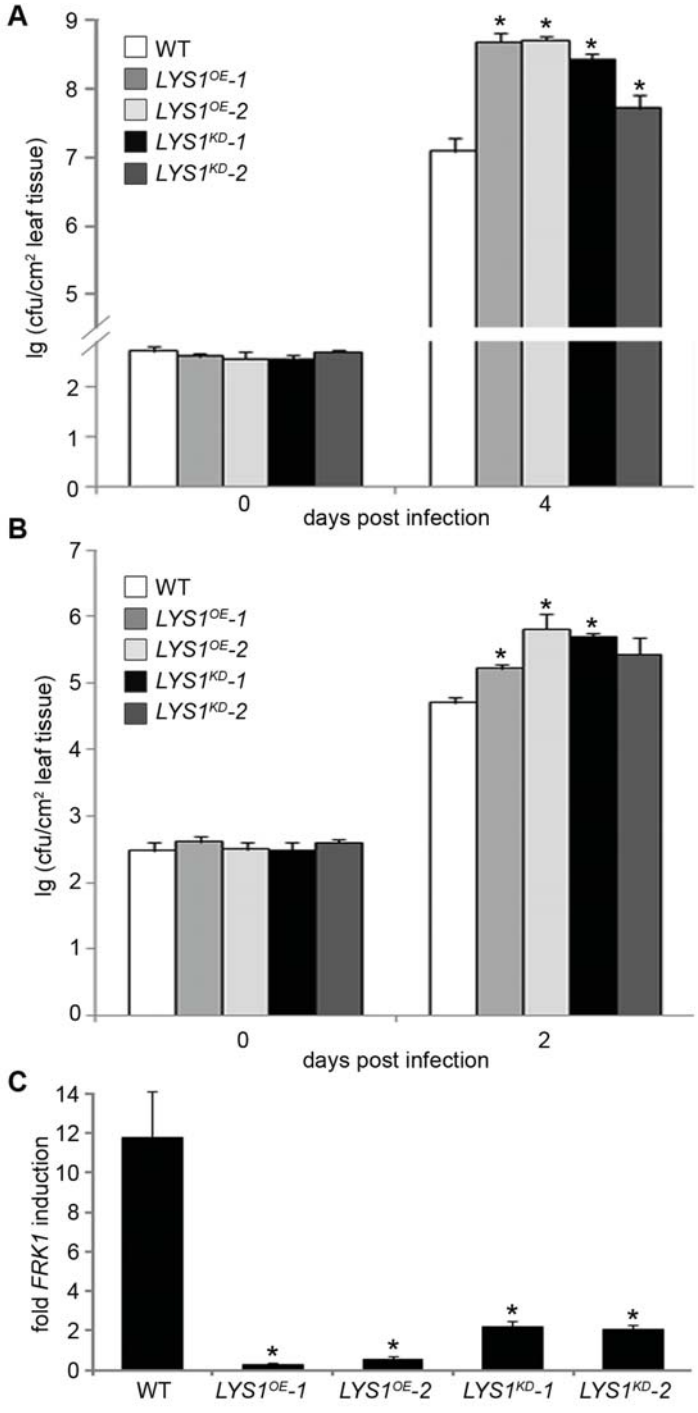
A
lg (cfu/cm² leaf tissue)
WT
LYS1OE-1
LYS1OE-2
LYS1KD-1
LYS1KD-2
days post infection
B
lg (cfu/cm² leaf tissue)
days post infection
C
fold FRK1 induction
WT
LYS1OE-1
LYS1OE-2
LYS1KD-1
LYS1KD-2